Horizon-Layered Cosmology: From Black Hole Gravitational Collapse to Holographic Hierarchies

Anđelko Đermek

Abstract

This work develops a horizon-based reconstruction framework exploring whether gravitational collapse and black-hole horizon physics admit a consistent reinterpretation as the kinematic origin of an emergent cosmological spacetime. The approach is grounded in gravitational time dilation, black-hole thermodynamics, and holographic entropy bounds, and is presented as a conceptual and kinematic construction rather than a complete dynamical theory.

In Schwarzschild geometry, infalling matter approaches the event horizon only asymptotically in the external time governing causal communication. This motivates an operational description in which infalling quanta are incorporated through discrete Planck-scale updates on a stretched horizon, treated as a null-synchronized, information-bearing surface with finite causal throughput. Lateral lightlike adjacency enforces coherence across the horizon, while the ordered growth of the horizon provides a natural causal ordering that can be used to define an internal notion of time.

A kinematic mapping is constructed from this two-dimensional, null-ordered surface to an effective three-dimensional bulk description. Tangential adjacency supplies transverse spatial structure, generational layering defines an effective radial coordinate, and global retessellation establishes temporal ordering. Under these assumptions, the reconstructed interior admits a homogeneous and isotropic Friedmann–Lemaître–Robertson–Walker envelope with coasting expansion $\boldsymbol{H(t) \sim 1/t}$ and an internal age of order $\boldsymbol{\sim 13.4\,\mathrm{Gyr}}$.

When the parent black hole carries angular momentum, Kerr-induced azimuthal phase gradients across the horizon encoding provide a possible geometric origin for large-scale parity-violating correlations and preferred axes. Quantum randomness is interpreted as arising from coarse-grained access to underlying boundary dynamics rather than from intrinsic indeterminism.

In this framework, the event horizon is reinterpreted not as a passive geometric boundary but as an actively evolving causal encoding surface whose null-ordered structure supports an emergent interior spacetime description.

Keywords: black hole; Schwarzschild geometry; holography; cosmology, FRW geometry

1 Introduction and Preface

Preface. This work is presented not as a final theory or a complete physical model, but as an exploratory framework intended to probe alternative ways of interpreting gravitational collapse and cosmological origin through a single informational principle. Many elements of the proposal extend beyond established theory, and no claim is made that all constructions described here correspond directly to realized physical processes.

Nevertheless, the framework is internally coherent and is motivated by well-known features of general relativity, black-hole thermodynamics, and holographic bounds. It seeks to examine whether these ingredients, when taken seriously and combined consistently, suggest a reinterpretation of horizons not merely as geometric boundaries but as *generative surfaces* from which spacetime, matter, and causal structure may emerge.

The central idea explored is that the event horizon plays an active, dynamical role in encoding and organizing physical degrees of freedom, and that its growth and causal ordering may admit an effective internal cosmological description. If correct even in part, this perspective would suggest that black holes could seed self-contained internal universes and that our own cosmos might be understood as such a holographically projected interior.

The purpose of this paper is therefore not to assert definitive conclusions, but to present a set of interconnected ideas that may be of conceptual interest and potential heuristic value. The constructions offered here are intended to stimulate discussion, identify possible avenues for further investigation, and clarify which aspects of the proposal could, in principle, be sharpened, challenged, or falsified within a more complete theoretical framework.

Introduction.

Black holes lie at the intersection of general relativity, quantum theory, and thermodynamics, and continue to expose deep tensions between geometric descriptions of spacetime and informational constraints. In classical general relativity, gravitational collapse generically leads to spacetime singularities hidden behind event horizons. While mathematically consistent within the classical framework, this picture leaves unresolved conceptual questions concerning the fate of information, the physical status of causally inaccessible regions, and the operational meaning of spacetime inside a horizon.

This work develops a horizon-based reconstruction framework that adopts an explicitly external, asymptotic viewpoint. In the Schwarzschild description, gravitational time dilation causes infalling matter to approach the event horizon only asymptotically in the time variable governing causal communication with the surrounding universe. Although a freely falling observer reaches the horizon in finite proper time, this proper-time description does not define a persistent causal ordering accessible to exterior observers: signals exchanged between the infalling matter and the asymptotic region become increasingly redshifted, and horizon crossing is never completed within finite external time.

From this operational perspective, infalling matter does not enter a new, independently evolving spacetime region. Instead, it is progressively incorporated into a thin, Planck-scale *stretched horizon* located just outside the Schwarzschild radius. Radial motion effectively freezes under extreme redshift, while tangential, lightlike propagation along the horizon remains operative. The physically relevant degrees of freedom associated with collapse are therefore organized into a two-dimensional, null surface endowed with causal structure and finite information capacity.

Gravitational collapse is thus reinterpreted not as continued volumetric contraction toward a central singularity, but as a surface-driven process of *causal incorporation*. Infalling quanta are assimilated into successive horizon-localized layers, each incorporated only after lateral causal coherence is established across the surface. The horizon grows outward through a sequence of completed Planck-scale updates, each encoding a finite increment of mass–energy consistent with holographic entropy bounds. In this framework, the event horizon is not merely a passive geometric boundary but an active encoding surface whose ordered evolution supplies the data from which an effective interior spacetime description may be reconstructed.

Early formulations of the holographic principle, from 't Hooft [1] and Susskind [2] to the membrane paradigm [3], emphasized the thermodynamic role of horizons and the area scaling of entropy. AdS/CFT duality [4] provided a precise correspondence between bulk and boundary descriptions in highly symmetric settings, but did not specify a causal, time-ordered mechanism by which infalling matter becomes dynamically encoded on a horizon. More recent quantum informational approaches employing tensor networks and error-correcting codes have clarified the algebraic structure of holography, while leaving the physical process of encoding and spacetime reconstruction largely implicit.

The present framework focuses on this encoding process itself. The horizon is modeled as a discrete null surface composed of Planck-area elements arranged in an approximately hexagonal tessellation, with unavoidable topological defects required by spherical geometry. These elements support local degrees of freedom that encode both cumulative horizon growth and laterally propagating field data. Infalling matter is represented operationally through horizon-localized excitations, while lateral null propagation at invariant speed c enforces global causal coherence during each completed incorporation.

A central construction of this work is a kinematic mapping between the two-dimensional horizon data and an effective three-dimensional interior geometry. Tangential adjacency on the horizon supplies transverse spatial structure, while the ordered sequence of incorporations defines an effective radial coordinate associated with cumulative information content rather than with a Schwarzschild distance. The resulting interior description admits a homogeneous and isotropic Friedmann–Lemaître–Robertson–Walker envelope with a coasting expansion law $H(t) \sim 1/t$, where cosmic time is identified with the ordered sequence of completed horizon updates rather than with an external background parameter.

Within this picture, the classical spacetime singularity is not realized as a physical endpoint. Once collapse reaches holographic saturation, further evolution is governed by horizon growth and boundary encoding rather than by continued compression of an

interior volume. The interior spacetime, when described at all, is a reconstructed, effective domain whose geometry is fully fixed by horizon data and carries no independent degrees of freedom beyond those encoded on the boundary.

If the parent black hole carries angular momentum, Kerr frame dragging induces azimuthal phase structure across the horizon. This rotational memory provides a geometric mechanism by which parity-violating correlations or preferred axes may be imprinted on large-scale modes of the reconstructed interior. Such effects, if present, would arise from horizon geometry and causal ordering rather than from inflationary initial conditions, and are therefore expected to be confined to the largest observable scales.

Scope and interpretation.

The framework developed here is intended as a kinematic and conceptual construction rather than a complete theory of quantum gravity. It does not replace the standard model of particle physics or derive the full dynamical content of Einstein's equations from microscopic rules. Instead, it explores whether gravitational collapse, holographic bounds, and causal structure admit a self-consistent reinterpretation in which horizons act as generative surfaces for effective spacetime descriptions.

Taken together, these considerations support a unified interpretive picture: gravitational collapse proceeds through ordered horizon growth rather than singularity formation; the event horizon functions as an information-bearing causal surface rather than a passive boundary; and the observable universe may be understood as an effective interior spacetime reconstructed from horizon-governed dynamics. In this view, the horizon is not the end of physics, but the interface through which spacetime structure emerges.

2 Schwarzschild Black Hole

The classical description of gravitational collapse originates from general relativity's prediction that sufficiently massive stars, once all pressure support is exhausted, undergo irreversible contraction. In the Schwarzschild solution, which describes a static, spherically symmetric vacuum spacetime, formal extension of the metric to $r = 0$ leads to a curvature singularity [5]. This singular behavior signals a breakdown of the classical description rather than a physically accessible endpoint of collapse.

A standard result of classical general relativity is that a freely falling observer reaches the Schwarzschild radius $r = 2M$ in a finite amount of proper time τ, while the Schwarzschild coordinate time t measured by a stationary observer at infinity diverges. This disparity is commonly addressed by introducing alternative coordinate systems, such as Kruskal–Szekeres coordinates, in which the metric is manifestly regular at $r = 2M$ and timelike geodesics extend smoothly across the horizon [6]. Such reparameterizations demonstrate that the horizon is not a curvature singularity and that local physics along the infalling worldline remains well behaved.

However, the removal of the coordinate singularity does not alter the operational fact that, when described in Schwarzschild time, the infalling trajectory approaches $r = 2M$ only asymptotically. The Schwarzschild time coordinate is tied to the proper time of observers at spatial infinity and therefore governs causal communication with the exterior universe. Relative to this external clock, the approach to the horizon is assigned an unbounded duration.

Despite this, the conventional interpretation emphasizes that the infalling particle must pass to smaller radii because its own proper time remains finite and the local geometry is smooth at the horizon [6]. Yet all physical observation accessible to distant observers is necessarily mediated by signals that propagate outward. Photons, neutrinos, and gravitational waves emitted from progressively smaller radii experience ever-increasing redshift, and every causal influence reaching infinity does so at a rate that slows without bound when measured against the external clock.

Gravitational redshift and time dilation are not merely coordinate conventions but experimentally verified physical effects. They have been confirmed with high precision in the Hafele–Keating circumnavigation experiment [7], in the relativistic timing corrections required for GPS satellite synchronization [8], and in modern optical clock tests [9]. These observations establish that time dilation directly affects physical rates as measured by observers in different gravitational potentials. In the context of collapse, this implies that the divergence of external time near the horizon has genuine operational meaning for the causal accessibility of infalling matter.

The special physical status of the horizon is further emphasized by black-hole thermodynamics. The Bekenstein–Hawking entropy depends on the area of the event horizon,

$$S_{\mathrm{BH}} = \frac{k_B c^3}{4G\hbar}\, A, \tag{1}$$

rather than on the volume of any interior region [10]. This identifies the horizon as the locus where information relevant to the external universe is encoded. Hawking radiation [11] reinforces this viewpoint: the emission originates in the near-horizon

region, and its properties are governed by surface gravity and horizon geometry, not by details of a putative interior.

Taken together, these considerations expose a genuine tension in the classical interpretation of collapse. While proper-time geodesics admit a smooth extension across the horizon, all empirically accessible quantities measured in the external frame indicate that the horizon is approached only asymptotically in the time variable that controls causal communication with the rest of the universe. Any physically complete description of gravitational collapse must therefore reconcile the regularity of local infall with the unbounded temporal delay experienced by external observers. This tension motivates a more careful analysis of infall in Schwarzschild geometry, to which we now turn.

2.1 Radial Free Fall

The radial motion of freely falling objects in the Schwarzschild geometry is governed by the temporal, radial, and angular components of the metric [12, p. 108]. For a non-rotating, uncharged black hole of mass M, the Schwarzschild line element in geometric units ($G = c = 1$) is

$$ds^2 = -\left(1 - \frac{2M}{r}\right) dt^2 + \left(1 - \frac{2M}{r}\right)^{-1} dr^2 + r^2 \left(d\theta^2 + \sin^2\theta \, d\phi^2\right). \tag{2}$$

Although the temporal and radial coefficients diverge as $r \to 2M$, the angular part of the metric remains finite. This asymmetry between radial and tangential behavior in the near-horizon region plays a central role in the causal structure of Schwarzschild spacetime and will be revisited in later sections.

For a particle released from rest at a finite radius r_0, the proper time experienced while falling to a radius r is

$$\tau - \tau_0 = \frac{2}{3\sqrt{2M}} \left(r_0^{3/2} - r^{3/2}\right), \tag{3}$$

a standard result obtained from the timelike geodesic equations [12, p. 221]. In contrast, the Schwarzschild coordinate time interval measured by a distant observer is [12, p. 219]

$$\begin{aligned} t - t_0 = &-\frac{2}{3\sqrt{2M}} \left[r^{3/2} - r_0^{3/2} + 6M\left(\sqrt{r} - \sqrt{r_0}\right)\right] \\ &+ 2M \ln\left(\frac{(\sqrt{r} + \sqrt{2M})(\sqrt{r_0} - \sqrt{2M})}{(\sqrt{r_0} + \sqrt{2M})(\sqrt{r} - \sqrt{2M})}\right). \end{aligned} \tag{4}$$

The logarithmic term diverges for $r \to 2M$, indicating that no particle crosses the event horizon in finite Schwarzschild coordinate time.

To analyze this divergence, let

$$r = 2M + u, \qquad u \ll 2M.$$

Expanding $\sqrt{r}$ around $2M$ gives

$$\sqrt{r} - \sqrt{2M} \;\approx\; \frac{u}{2\sqrt{2M}}, \tag{5}$$

so the denominator in the logarithm of §(4) approaches zero linearly in u, producing the divergence in t as $u \to 0$.

The proper radial distance corresponding to a coordinate displacement dr near the horizon is

$$ds_r = \frac{dr}{\sqrt{1 - \frac{2M}{r}}} \;\approx\; \sqrt{\frac{2M}{u}}\, dr, \tag{6}$$

since $1 - 2M/r \approx u/(2M)$ when $u \ll 2M$. For an object of fixed proper radial length l_0, the corresponding coordinate length is therefore

$$\Delta r \;\approx\; l_0 \sqrt{\frac{u}{2M}}, \tag{7}$$

which shrinks to zero as $u^{1/2}$ when the horizon is approached. This near-horizon contraction is independent of the black hole mass.

The coordinate-time evolution of $u = r - 2M$ may be obtained from the radial geodesic equation for infall from rest at r_0 (see [13, p. 227]):

$$\frac{dr}{dt} = -\left(1 - \frac{2M}{r}\right)\sqrt{\frac{2M}{r}}. \tag{8}$$

Near the horizon, $\sqrt{2M/r} \approx 1$, so

$$\frac{du}{dt} = \frac{dr}{dt} \;\approx\; -\frac{u}{2M}. \tag{9}$$

Integrating gives

$$\ln\left(\frac{u_2}{u_1}\right) = -\frac{\Delta t}{2M}. \tag{10}$$

For a halving of the remaining radial distance, $u_2 = u_1/2$, one obtains

$$\Delta t = 2M \ln 2. \tag{11}$$

Thus the Schwarzschild coordinate time required to reduce the radial offset by a fixed fraction is proportional to the black hole mass.

Numerically, using $M_\odot \simeq 1.48 \times 10^3\,\mathrm{m}$ in geometric units,

$$\begin{aligned} M = 100M_\odot: &\quad \Delta t \approx 6.826 \times 10^{-4}\,\mathrm{s}, \\ M = 1M_\odot: &\quad \Delta t \approx 6.826 \times 10^{-6}\,\mathrm{s}. \end{aligned} \tag{12}$$

§(11) expresses the familiar logarithmic divergence of Schwarzschild time as the horizon is approached. Each halving of the remaining distance requires the same additional coordinate time, leading to a Zeno-like accumulation of delays reminiscent of the classical paradox of infinite subdivision [14].

Despite this divergence in t, the proper time to reach $r = 2M$ remains finite, as §(3) shows. The divergence in §(4) becomes significant only within a microscopically small interval extremely close to the horizon. Consequently, from the viewpoint of a distant observer, infalling matter approaches a region just outside the horizon (on scales far below any astrophysical resolution) within a short coordinate time, even though the horizon itself is never crossed in finite t.

2.2 External Observer versus Infalling Observer Experience

The Schwarzschild geometry exhibits a well-known disparity between the description of infalling matter provided by stationary observers at large radius and the description along the infalling worldline itself. Both descriptions arise from the same spacetime metric, but they employ different notions of time: the Schwarzschild coordinate time t, which coincides with the proper time of static observers at infinity, and the proper time τ measured along the infalling trajectory. This distinction is central to the causal and operational structure of black-hole spacetimes.

External stationary observer. As shown in §(4), the Schwarzschild coordinate time required for an infalling particle to reach radius r diverges logarithmically as $r \to 2M$,

$$t \;\to\; +\infty \qquad \text{as} \qquad r \to 2M. \tag{13}$$

Consequently, a stationary observer at infinity never records a completed horizon-crossing event at any finite value of t. All signals emitted from increasingly near the horizon arrive with arbitrarily large redshift and delay. The gravitational redshift factor for clocks held at fixed radius,

$$\sqrt{1 - \frac{2M}{r}}, \tag{14}$$

tends to zero as $r \to 2M$, producing an effective freeze-out of all near-horizon processes in the external description. This behavior reflects an operational fact: no finite exterior time suffices to resolve dynamics arbitrarily close to the horizon.

Infalling observer. Along a freely falling worldline, the proper time required to reach the horizon from any $r_0 > 2M$ is finite, as given by §(3). The continuation of the infalling trajectory across $r = 2M$ is smooth in terms of local curvature invariants

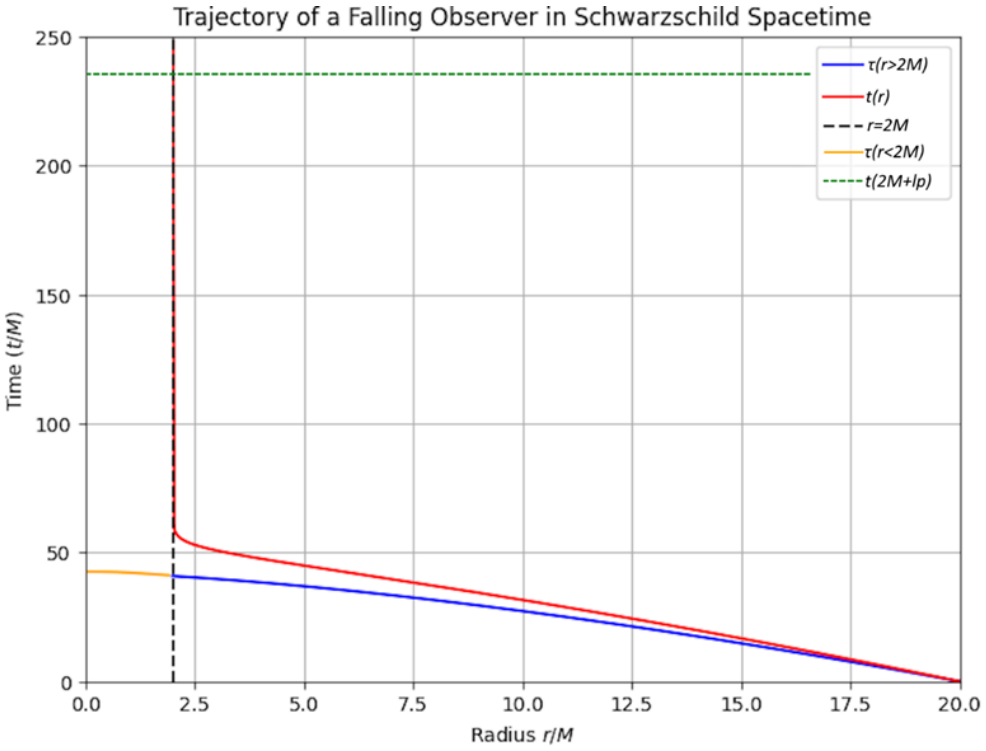

Fig. 1 The trajectory of a radially infalling observer in Schwarzschild spacetime plotted in terms of both proper time τ §(3) and Schwarzschild coordinate time t §(4). Both trajectories begin at $r_0 = 20M$, with $t_0 = \tau_0 = 0$. The orange segment represents a continuation of the proper time trajectory past the horizon. The green line indicates the coordinate time at which the infaller reaches a Planck-length distance from the horizon. Adapted from [12].

and proper time. However, the relation between τ and the exterior time t is highly nonlinear: for a radial geodesic with conserved energy per unit mass E,

$$\frac{dt}{d\tau} = \frac{E}{1 - \frac{2M}{r}}, \tag{15}$$

which diverges as $r \to 2M$. Thus, although the infaller experiences no local pathology, the exterior time coordinate ceases to provide a faithful parametrization of the infalling worldline near the horizon.

Operational interpretation. The divergence of t at $r = 2M$ should not be interpreted as a breakdown of local physics, but it has a clear operational consequence: *no exterior observer can assign a finite time label to a completed horizon-crossing event.* From the perspective of exterior physics, the approach to the horizon is an asymptotic process that is never operationally completed within any finite interval of Schwarzschild time. Accordingly, the horizon functions as a causal boundary for the

external description, even though the spacetime metric admits a formal continuation beyond it.

Evaporation and finite exterior lifetime. If semiclassical effects such as Hawking evaporation are taken into account, the exterior geometry is no longer stationary. In such cases the lifetime of the black hole, as measured in the exterior time t, is finite. Since horizon crossing requires $t \to \infty$ in the stationary approximation, no completed crossing event can be realized within the finite exterior lifetime of an evaporating black hole. The infalling worldline instead asymptotically approaches a shrinking trapping region, while exterior observers describe the interaction in terms of near-horizon absorption, redshift, and outgoing flux.

A number of semiclassical analyses support the view that horizon formation and traversability are not guaranteed once backreaction is included [15–19]. In these approaches, the physically relevant boundary for exterior dynamics is a trapping or stretched horizon rather than a completed global event horizon.

Consequences. For all processes describable within finite exterior time, infalling matter is effectively absorbed, thermalized, and encoded at the stretched horizon. Although the classical metric allows a formal continuation of geodesics beyond $r = 2M$, such continuation has no operational realization in the exterior causal description. Exterior physics is therefore complete when formulated in terms of horizon degrees of freedom, without requiring access to an interior region.

Within any finite interval of exterior time, no horizon-crossing event is operationally realized. All observable infalling matter remains arbitrarily close to $r = 2M$, and the stretched horizon provides the effective locus of exterior dynamics and information storage.

3 Event Horizon and Local Horizon Formation

From the earliest collapse models of Oppenheimer and Snyder (1939) to modern numerical simulations, the *event horizon* of a black hole is understood as a global, teleological construct: it is defined as the boundary separating null geodesics that eventually escape to infinity from those that do not, and can be identified only after the entire spacetime evolution is known. By contrast, the horizons that arise dynamically during collapse, apparent, trapping, or dynamical horizons, are locally defined and admit a causal, time-dependent description. In what follows, we focus on these local horizons, which govern the physical process of collapse at finite time and underlie the effective exterior description.

In classical general relativity, a necessary condition for the formation of a locally trapped region in a spherically symmetric spacetime is the compactness inequality

$$\frac{2G\,m(r)}{r\,c^2} \;\geq\; 1, \tag{16}$$

where $m(r)$ is the mass enclosed within areal radius r. Expressed in terms of the mean density,

$$\langle \rho(r) \rangle = \frac{3\,m(r)}{4\pi r^3}, \tag{17}$$

this condition becomes the lower bound [20]

$$\langle \rho(r) \rangle \;\geq\; \frac{3c^2}{8\pi G r^2}. \tag{18}$$

The required mean density therefore increases rapidly as r decreases, implying that trapped surfaces generically form first in the densest central regions of a collapsing object.

Numerical simulations of stellar collapse confirm this behavior: only a fraction (typically $\sim$ 5–25%) of the final black-hole mass lies within the initially formed trapped or apparent horizon, while additional mass is incorporated as the horizon expands outward [21–23]. Thus, while the global event horizon is defined teleologically, the locally defined horizon relevant to collapse dynamics forms at small radii and grows continuously as further layers of matter satisfy the compactness condition.

To formalize this behavior, define the local compactness function

$$f(r) = \frac{2G\,m(r)}{r\,c^2}, \tag{19}$$

with

$$m(r) = 4\pi \int_0^r \rho(r')\, r'^2\, dr'. \tag{20}$$

For any nonnegative density profile $\rho(r) \geq 0$, $m(r)$ is monotonic. Differentiation yields

$$f'(r) = \frac{2G}{c^2}\left(4\pi r\,\rho(r) - \frac{m(r)}{r^2}\right) = \frac{2G}{c^2}\,\frac{d}{dr}\left(\frac{m(r)}{r}\right). \tag{21}$$

Hence $f(r)$ increases with radius wherever the local density exceeds the interior average. During realistic collapse, the core typically develops the strongest overdensity, so the condition $f(r) = 1$ is first satisfied in a small central region and subsequently propagates outward, describing the growth of a trapped surface.

This inside-out growth is consistent with the dynamics of gravitational collapse. If most of the mass were confined to a thin outer shell with negligible interior mass, the shell would experience only weak inward acceleration,

$$a(R) \approx -\frac{G\,m(R_{\text{inner}})}{R^2}, \tag{22}$$

and would require finely tuned initial conditions to satisfy §(16) at its own radius. Realistic collapse solutions instead develop a central overdensity that naturally drives early horizon formation at small r, followed by outward expansion as additional matter is incorporated.

In the horizon-layered interpretation, this classical picture admits a natural holographic parametrization. The Planck scale marks the regime in which the compactness condition becomes order unity for minimal mass concentrations, signaling the breakdown of a purely classical description. Rather than implying a literal pointlike collapse, this suggests that the earliest trapped region is associated with Planck-scale physics, beyond which additional mass–energy increases the area of the horizon. In this sense, the growth of the local horizon may be viewed as proceeding in successive layers, consistent with the area scaling of gravitational entropy.

In summary, while the global event horizon is a teleological construct defined only after the full spacetime history is known, the physically relevant horizon during collapse is a locally defined trapped or apparent horizon. Such horizons form causally in the densest central regions and expand outward as additional matter satisfies the compactness condition. This dynamical, inside-out growth provides the appropriate foundation for a boundary-based, holographic description of black-hole formation and evolution.

3.1 Formation of the Planck Seed and the Onset of Horizon Layering

Locally defined trapped horizons form at the smallest radius where the compactness condition is satisfied. As gravitational collapse drives the core density toward the Planck regime, a minimal trapped region is expected to nucleate, marking the onset of horizon formation in the local, quasi-classical description. Subsequent accretion increases the enclosed mass $m(r)$, causing the locus where $2Gm(r)/(rc^2) = 1$ is satisfied to move outward through a sequence of nested null surfaces. In this sense, the

horizon relevant to collapse dynamics is not a pre-existing geometric boundary but a causally generated surface that expands as additional mass–energy is incorporated.

The threshold for local horizon formation follows directly from the compactness criterion,

$$\langle \rho(r) \rangle \;\geq\; \frac{3c^2}{8\pi G r^2}, \tag{23}$$

which is obtained by rewriting the Schwarzschild condition $2Gm(r)/(rc^2) \geq 1$ in terms of the mean density. To estimate the scale at which this condition is first met, one may compare the required density with that of a configuration containing a single Planck mass,

$$\rho_{\mathrm{p}}(r) = \frac{m_{\mathrm{p}}}{\frac{4}{3}\pi r^3}, \tag{24}$$

where $m_{\mathrm{p}} = \sqrt{\hbar c/G}$. Equating $\rho_{\mathrm{p}}(r) = \frac{3c^2}{8\pi G r^2}$ yields

$$r_{\mathrm{crit}} = \frac{\ell_{\mathrm{p}}}{\sqrt{2}}, \tag{25}$$

which is of order the Planck length. This estimate should be understood as an order-of-magnitude indication that the first trapped region forms when densities approach the Planck scale, rather than as a literal microphysical collapse to a pointlike object.

Once such a minimal trapped region forms, continued collapse is no longer adequately described as further three-dimensional compression of an interior volume. Instead, additional mass–energy primarily increases the area of the trapped surface, shifting the radius at which $2Gm(r)/(rc^2) = 1$ is satisfied outward. The collapse thus transitions from a volumetric description to one in which the growth of a null boundary captures the dominant gravitational dynamics. This marks the onset of what we refer to as *horizon layering*.

The commonly quoted Planck density,

$$\rho_{\mathrm{P}}^{(\mathrm{std})} = \frac{m_{\mathrm{p}}}{\frac{4}{3}\pi \ell_{\mathrm{p}}^3} \simeq 5 \times 10^{96}\,\mathrm{kg/m^3}, \tag{26}$$

arises from assigning a Euclidean volume to a Planck-scale region. At such scales, however, classical notions of volume lose operational meaning, and the compactness condition provides a more physically motivated criterion. Using $r_{\mathrm{crit}} = \ell_{\mathrm{p}}/\sqrt{2}$ instead yields

$$\rho_{\mathrm{P}}^{(\mathrm{crit})} = \frac{m_{\mathrm{p}}}{\frac{4}{3}\pi r_{\mathrm{crit}}^3} \simeq 1.2 \times 10^{96}\,\mathrm{kg/m^3}, \tag{27}$$

which differs only by an order-unity factor but corresponds directly to the onset of local horizon formation.

In this picture, every black hole, regardless of its final macroscopic mass, originates from a trapped region whose characteristic scale is set by Planckian physics. Large black holes do not appear instantaneously at macroscopic radii; they grow outward as successive layers of infalling matter satisfy the compactness condition. The resulting

horizon can be viewed as a layered null surface whose area increases in accordance with the incorporation of mass–energy, consistent with the holographic scaling of gravitational entropy.

Within the horizon-layered framework, the classical singularity predicted by general relativity is not realized as a physical endpoint. Instead, the approach to Planckian densities signals a transition to a regime in which collapse is regulated by horizon growth and boundary encoding. The would-be singular region is replaced by a finite trapped core whose further evolution is captured by the expansion of the horizon, preserving unitarity and maintaining consistency with holographic entropy bounds throughout the collapse process.

3.2 Causal Exclusion, Horizon Encoding, and the Status of the Interior

As a locally defined trapped or dynamical horizon forms and grows outward from Planckian scales, a natural question arises: *what is the physical status of the spacetime region that the horizon appears to enclose?* From the asymptotic observer's perspective, the answer is operationally clear. All physically accessible information associated with the black hole is encoded at, or arbitrarily close to, the horizon, while the exterior spacetime remains causally and informationally complete. No observation available to exterior observers requires access to, or influence from, a region behind the horizon. In this precise operational sense, the interior may be treated as a causally excluded domain without independent physical degrees of freedom.

In the classical geometric picture, the horizon is often regarded as a passive boundary surrounding a pre-existing interior manifold that continues to evolve independently. Within the horizon-layered framework, this intuition is replaced by a holographically motivated interpretation grounded in entropy bounds, causal accessibility, and the external description of black-hole dynamics.

The interior is not an ontologically independent region of spacetime. Its effective geometry, when introduced, is a reconstructed description fixed entirely by the information encoded on the horizon.

Classical general relativity predicts that, under broad conditions, continued gravitational collapse leads to spacetime singularities characterized by geodesic incompleteness and divergent curvature invariants. If such singular regions were regarded as physically real domains carrying independent degrees of freedom, they would permit the concentration of arbitrarily large information content into regions of vanishing boundary area. This would violate the Bekenstein–Hawking entropy relation and the covariant entropy bound [24], which constrain the maximal entropy of any causally complete region to

$$S_{\max} = \frac{A}{4\,\ell_{\mathrm{p}}^2}, \tag{28}$$

where A is the area of an appropriate bounding surface.

From a holographic standpoint, the appearance of a singularity therefore signals not the physical realization of infinite curvature or information density, but the breakdown of a purely volumetric bulk description beyond its regime of applicability. When collapse approaches holographic saturation, the correct physical description must reorganize degrees of freedom onto a boundary encoding in order to preserve causal and informational consistency.

In the horizon-layered framework, this reorganization is realized through the formation and growth of locally defined horizons. As mass–energy is absorbed, the horizon expands and its area increases, providing the additional information capacity required to maintain consistency with holographic entropy bounds. At any stage of collapse, the maximal information content is therefore

$$I_{\max}(t) = \frac{A(t)}{4\,\ell_{\mathrm{p}}^2}, \tag{29}$$

with the growth of $A(t)$ tracking the causal incorporation of new degrees of freedom. This should be understood as an effective holographic bookkeeping of physical information, not as a literal discretization of spacetime microstructure.

Once a trapped surface forms, the region behind it becomes causally excluded from the exterior description. All information accessible to asymptotic observers about the black hole, its mass, entropy, angular momentum, and subsequent evolution, is encoded at the horizon. Accordingly, the horizon is not a passive geometric divider but an *active, information-bearing null surface* whose successive updates fix the entire physically relevant description of the system.

This conclusion is reinforced by the operational status of horizon crossing and Hawking radiation. In the classical metric extension, an infalling particle is said to cross the event horizon and enter an interior spacetime region. However, for external observers, horizon crossing is never completed within any finite interval of the exterior time variable governing causal communication with infinity. Signals exchanged with the infalling system become arbitrarily redshifted, and all information associated with the infaller is effectively absorbed into the horizon encoding. The horizon therefore functions as the terminal surface of the exterior effective description.

This viewpoint does not modify the standard semiclassical account of Hawking radiation. Hawking radiation arises from quantum field theory in the exterior spacetime and from the mismatch between vacuum definitions at past and future null infinity. It is generated by vacuum polarization effects in the near-horizon region, where strong gravitational redshift distorts field modes arbitrarily close to the horizon. The near-horizon geometry is locally Rindler-like, and it is this universal kinematic structure that underlies the thermal character of the radiation.

For a static observer at radius r, the asymptotic energy of a quantum emitted from the near-horizon region is related to its locally measured energy by

$$E_\infty = E_{\mathrm{local}}\sqrt{1 - \frac{2Gm_{\mathrm{bh}}}{rc^2}}, \tag{30}$$

and in the near-horizon limit this yields the Hawking temperature

$$T_H = \frac{\hbar c^3}{8\pi G m_{\rm bh} k_B}. \tag{31}$$

These relations depend only on the exterior geometry and surface gravity and do not require assigning physical degrees of freedom to a resolved interior region.

Energy conservation is implemented entirely at the level of the horizon. Outgoing modes that carry positive energy to infinity are accompanied by a corresponding decrease in the mass and area encoded on the horizon. What is often described heuristically as an inward flux of negative energy is more precisely understood as a boundary bookkeeping relation within the exterior effective theory. Black-hole evaporation is therefore a gradual depletion of horizon-encoded degrees of freedom, fully captured without reference to interior dynamics.

This resolves a key conceptual point: if the interior possessed independent physical degrees of freedom, there would be no consistent mechanism by which black-hole mass and entropy could decrease, since no process observable from the exterior involves energy extraction from an interior region. The fact that black holes evaporate completely through horizon-mediated processes indicates that all physically relevant degrees of freedom are encoded on the horizon itself. When the horizon shrinks and ultimately disappears, so too does the associated interior reconstruction.

In this unified view, the interior spacetime of a black hole is not a fundamental entity but a derived, coarse-grained construct. Its apparent geometry reflects the layered information content and causal ordering of the horizon, and it acquires meaning only insofar as such a reconstruction is useful. Where classical general relativity predicts singular behavior, the holographic description replaces it with boundary reorganization and horizon evolution, preserving unitarity, entropy bounds, and causal completeness without invoking physical singularities or independently evolving interior regions.

3.3 Reinterpretation of Mass and Spacetime

In classical general relativity, gravitational collapse leads, under broad assumptions, to spacetime singularities characterized by geodesic incompleteness and divergent curvature invariants, as formalized in the Penrose–Hawking singularity theorems [25]. These results are derived within a framework that assumes a smooth spacetime manifold and the validity of the classical Einstein field equations,

$$R_{\mu\nu} - \tfrac{1}{2} g_{\mu\nu} R = \frac{8\pi G}{c^4} T_{\mu\nu}. \tag{32}$$

In the horizon-layered holographic interpretation developed here, this equation is retained as an effective bulk description, while its source term admits a complementary boundary-based interpretation.

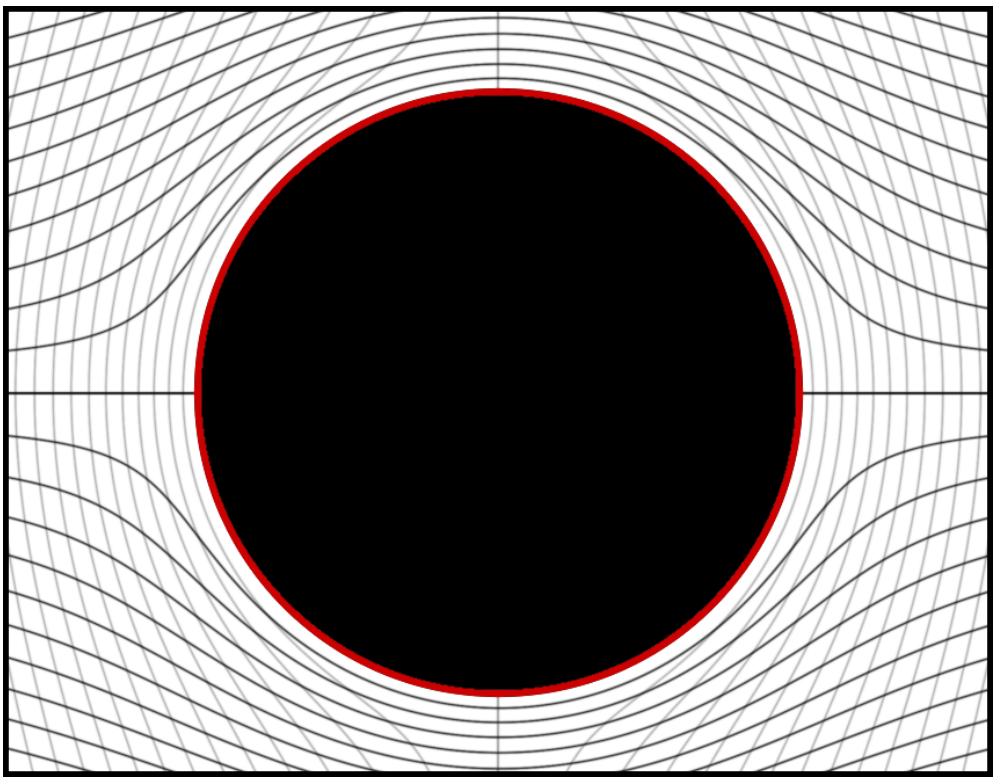

Fig. 2 Heuristic visualization of spacetime geodesics near a Schwarzschild black hole, illustrating an external-observer, horizon-centered interpretation. The bending of trajectories is shown in analogy with streamlines in a fluid flow, not as a literal dynamical mechanism. In this interpretive picture, the event horizon is treated as an operational boundary for reconstruction: interior spacetime is not directly modeled, and bulk geometry is inferred from horizon-side data. Geodesics that intersect the horizon correspond to trajectories entering a region that is causally inaccessible to the external description, while tangential geodesics remain entirely in the exterior. The horizon is depicted as an information-bearing surface encoding the inaccessible interior in a holographic sense. This figure is illustrative and does not represent a claim about modified geodesic equations or the literal absence of interior spacetime in classical general relativity.

Curvature as encoded causal structure. Rather than viewing curvature as arising from matter localized within an ontologically independent interior volume, the horizon-layered framework interprets stress–energy as characterizing how causal connectivity is redistributed at the boundary. A massive excitation corresponds to a localized reduction in available null connectivity, a *causal deficit*, that must be accommodated by curvature in the surrounding effective bulk geometry. Geodesics bend not because they orbit a material core hidden in the interior, but because the causal adjacency structure encoded on the horizon constrains the paths available to null and timelike propagation. In this sense, Einstein's equations function as macroscopic bookkeeping relations governing how bulk geometry responds to boundary-encoded causal constraints.

Horizon as the terminal surface of the exterior description. Within the exterior effective theory, the black-hole horizon functions as a terminal null boundary. All information accessible to exterior observers is encoded at, or arbitrarily close to, this surface. Although the classical metric admits a formal continuation beyond the horizon, the interior region is no longer independently specifiable in operational terms. Processes such as Hawking radiation, backreaction, and horizon growth are fully captured by exterior degrees of freedom. The interior spacetime, when discussed at all, is therefore understood as an emergent, reconstructed geometry derived from horizon data rather than as a fundamental arena of physics.

This viewpoint is naturally aligned with the holographic principle. The Bekenstein–Hawking entropy relation,

$$S = \frac{k_B c^3}{4\hbar G}\, A, \tag{33}$$

implies that the information content relevant to gravitational dynamics scales with area rather than volume. In the present interpretation, the stress–energy tensor $T_{\mu\nu}$ encodes not only conventional matter content but also the effective geometric response required to maintain consistency with boundary-imposed causal constraints. Newton's constant G quantifies the compliance of the bulk geometry to these constraints. Classical singular behavior arises when bulk evolution is extrapolated beyond the regime in which such a volumetric description remains meaningful, rather than from the physical realization of infinite density or curvature.

Effective membrane behavior of the horizon. With no independently evolving interior required to support it, the horizon is maintained entirely by exterior geometry and boundary encoding. In the sense captured by the membrane paradigm, the horizon behaves as a coarse-grained null membrane endowed with effective transport properties. External curvature tends to deform this surface, while its encoded degrees of freedom resist deformation in a manner consistent with entropy bounds. This membrane behavior is not fundamental microphysics but an effective description reflecting the fact that horizon stability is a boundary property rather than the result of interior support.

Causal connectivity as a unifying language. Within this framework, different physical components may be characterized by how they couple to the underlying causal network. Ordinary matter corresponds to excitations that retain full causal connectivity to gauge and quantum fields while inducing curvature through boundary encoding. Radiation corresponds to fully connected, massless excitations propagating along null directions. Vacuum structure reflects residual, delocalized causal capacity that manifests as quantum fluctuations when projected into the bulk. These identifications are interpretive and do not modify the standard model of particle physics; they provide a unifying geometric language for gravitational coupling rather than new dynamical postulates.

In this picture, the Planck mass,

$$m_{\mathrm{P}} = \sqrt{\frac{\hbar c}{G}}, \tag{34}$$

marks the scale at which boundary encoding and causal exclusion become self-sustaining. Below this scale, matter is well described as embedded in an effectively smooth spacetime. Above it, horizon formation signals a transition to boundary-dominated dynamics. Rest energy $E = mc^2$ acquires an effective geometric interpretation as the curvature cost of maintaining a persistent causal deficit, while kinetic energy corresponds to the redistribution of this cost across the null network.

In summary, mass, radiation, vacuum structure, and gravitational curvature admit a unified interpretation in terms of causal connectivity and boundary encoding. Einstein gravity is recovered as the effective bulk response to these boundary conditions. Classical singularities are not realized as physical entities but indicate the breakdown of an unconstrained volumetric description once holographic bounds become operative. The interior spacetime of a black hole is therefore not a fundamental object, but a derived construct whose apparent geometry reflects the evolving information content of the horizon.

3.4 Planck-Step Horizon Synchronization

Gravitational collapse enters a regime where further infall is no longer adequately described by classical timelike trajectories, and near-horizon redshift effects dominate the dynamics. Beyond this threshold, incoming matter–energy is not effectively modeled as continuing compression into a pre-existing volume, but instead by its transcription into horizon-localized degrees of freedom: angular-momentum eigenmodes, quantum fluctuations, and spin-network links that together form the black hole's holographic code. The "interior" is not an independently evolving spacetime region but an emergent, holographically reconstructed domain whose causal ordering is defined entirely by the stratified horizon surface. Although the internal volume scales as r_{s}^3, its causal and informational origin lies in the ordered sequence of null layers that expand the horizon.

The Schwarzschild radius of a black hole of mass m_{bh} is

$$r_{\mathrm{s}} = \frac{2G\, m_{\mathrm{bh}}}{c^2}, \tag{35}$$

so that a small mass increment Δm_{bh} produces a radial shift

$$\Delta r_{\mathrm{s}} = \frac{2G\, \Delta m_{\mathrm{bh}}}{c^2}. \tag{36}$$

For a Planck-mass increment,

$$\Delta m_{\mathrm{bh}} = m_{\mathrm{p}} \quad \Rightarrow \quad \Delta r_{\mathrm{s}} = 2\, \ell_{\mathrm{p}}. \tag{37}$$

Each Planck-mass increment therefore corresponds, at the level of dimensional bookkeeping, to a horizon displacement of order $2\ell_{\mathrm{p}}$. In the horizon-layered cosmology, such a displacement defines the smallest causally meaningful update of the horizon geometry: one effective tick of the holographic code.

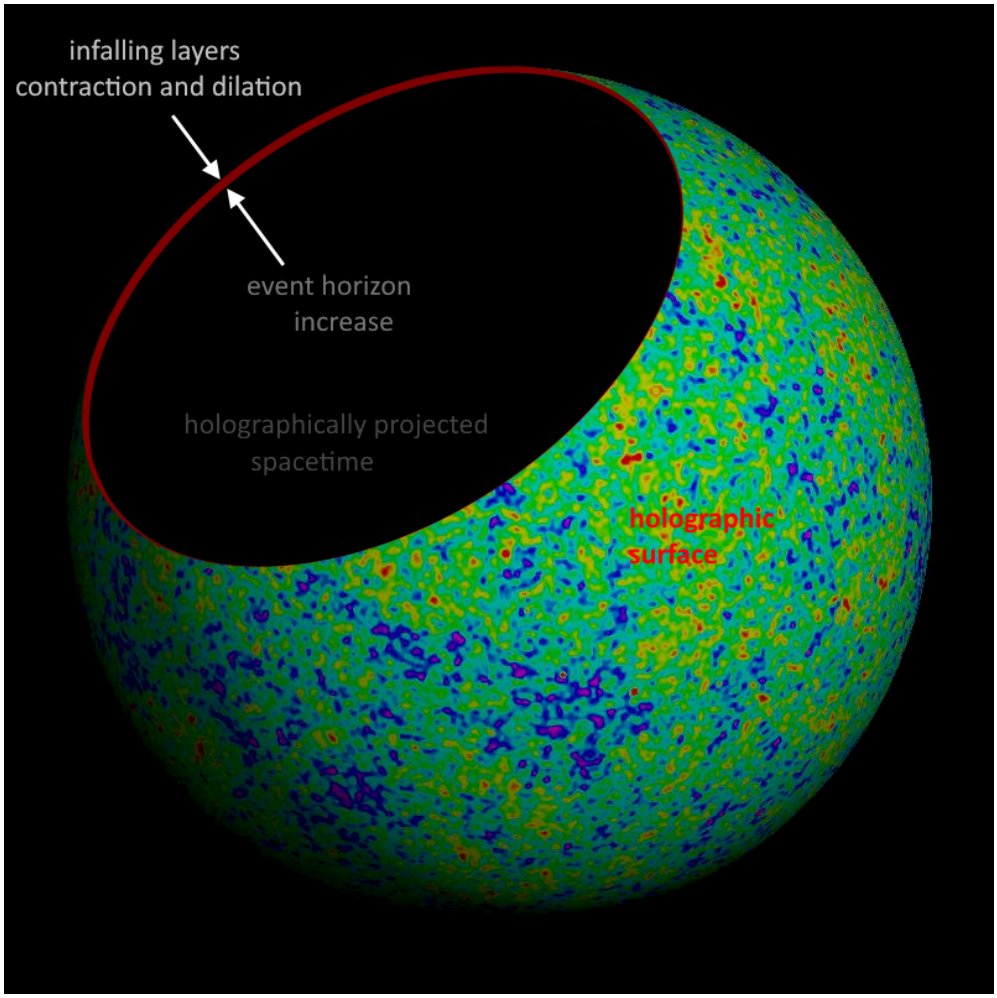

Fig. 3 Schematic representation of black hole gravitational collapse at a causal distance of ℓ_p above the event horizon. As infalling mass increases, the horizon expands, creating a redshift-based foliation of null layers just above the event horizon. Internal spacetime is a holographic projection.

The Planck quantities form the synchronized triplet

$$m_{\rm p} = \sqrt{\frac{\hbar c}{G}}, \qquad \ell_{\rm p} = \sqrt{\frac{\hbar G}{c^3}}, \qquad t_{\rm p} = \frac{\ell_{\rm p}}{c}, \tag{38}$$

linked by

$$\frac{G m_{\rm p}^2}{\ell_{\rm p}} = m_{\rm p} c^2 = \frac{\hbar}{t_{\rm p}}. \tag{39}$$

At this scale, gravitational self-energy, relativistic causality, and quantum uncertainty coincide, defining the smallest self-localized excitation compatible with both general

relativity and quantum mechanics. Accordingly, the synchronized triplet

$$(\Delta m,\, \Delta r,\, \Delta t) = (m_{\rm p},\, 2\ell_{\rm p},\, t_{\rm p}) \tag{40}$$

provides a natural causal bookkeeping unit for horizon growth.

The corresponding change in horizon area is

$$A = 4\pi r_{\rm s}^2 \quad \Rightarrow \quad \Delta A = 8\pi r_{\rm s}\, \Delta r_{\rm s} = 16\pi r_{\rm s}\, \ell_{\rm p}, \tag{41}$$

so that

$$\frac{\Delta A}{\ell_{\rm p}^2} = 16\pi\, \frac{r_{\rm s}}{\ell_{\rm p}} = 32\pi\, \frac{m_{\rm bh}}{m_{\rm p}}, \tag{42}$$

where the final equality follows from $r_{\rm s} = 2(m_{\rm bh}/m_{\rm p})\, \ell_{\rm p}$.

The holographic principle assigns a maximal information content

$$I_{\rm max} = \frac{A}{4\, \ell_{\rm p}^2}, \tag{43}$$

which in this framework is dynamically saturated and maintained by successive Planck-scale incorporations. Using

$$A = 16\pi\, \frac{G^2 m_{\rm bh}^2}{c^4}, \qquad \ell_{\rm p}^2 = \frac{\hbar G}{c^3}, \tag{44}$$

one finds

$$I = 4\pi \left(\frac{m_{\rm bh}}{m_{\rm p}} \right)^2, \tag{45}$$

with incremental information

$$\Delta I_{\rm p} = 8\pi\, \frac{m_{\rm bh}}{m_{\rm p}}. \tag{46}$$

The entropy follows the same law,

$$S_{\rm bh} = 4\pi k_{\rm B} \left(\frac{m_{\rm bh}}{m_{\rm p}} \right)^2, \tag{47}$$

with incremental entropy

$$\Delta S_{\rm p} = 8\pi k_{\rm B}\, \frac{m_{\rm bh}}{m_{\rm p}}. \tag{48}$$

In this framework, mass, entropy, and information emerge as complementary expressions of a single causal process: the sequential incorporation of null layers at the Planck-scale causal bandwidth $P_{\rm max} = c^5/G$. Each update increases $m_{\rm bh}$, A, S, and I in lockstep, maintaining exact holographic saturation,

$$S \propto I \propto A \propto m_{\rm bh}^2, \qquad \Delta S,\, \Delta I \propto m_{\rm bh}. \tag{49}$$

Planck-step horizon synchronization thus realizes bulk–boundary duality as an explicit causal bookkeeping mechanism, furnishing a singularity-free description of black-hole growth while preserving unitarity through horizon encoding.

The Planck-step description should be understood as an effective causal accounting scheme rather than a claim of fundamental discreteness of spacetime.

3.5 Radial Freezing and Null-Ordered Layering

As infalling matter approaches the near-horizon region, gravitational redshift and relativistic time dilation strongly suppress radial motion as described in Schwarzschild coordinates. For a near-radial null trajectory,

$$\frac{dr}{dt} = \pm\Big(1 - \frac{r_s}{r}\Big), \tag{50}$$

so that $dr/dt \to 0$ as $r \to r_s$. From the perspective of an external observer, any dynamical process requiring finite radial advance therefore becomes arbitrarily time-dilated as the horizon is approached.

To quantify the near-horizon behavior, write

$$r = r_s + \epsilon, \qquad \epsilon \ll r_s, \tag{51}$$

where ϵ is a coordinate offset used solely to parametrize proximity to the horizon. The Schwarzschild metric implies that a proper radial interval l_0 corresponds to a coordinate interval

$$\Delta r \simeq l_0 \sqrt{\frac{\epsilon}{r_s}}. \tag{52}$$

As $\epsilon \to 0$, the coordinate thickness of any structure with fixed proper size collapses toward zero. This behavior reflects the breakdown of Schwarzschild radial resolution near the horizon rather than a physical compression of matter to arbitrarily small proper scales.

In semiclassical treatments, the description of spacetime is expected to lose operational meaning below a proper distance of order the Planck length $\ell_{\rm p}$. Accordingly, we introduce a *stretched horizon* as an effective cutoff surface defined by the condition that its proper distance from the geometric horizon is of order $\ell_{\rm p}$. In Schwarzschild coordinates this corresponds parametrically to

$$\epsilon \sim \ell_{\rm p}, \tag{53}$$

up to factors of order unity. No claim is made that dynamics halt at this scale; rather, $\ell_{\rm p}$ marks the limit beyond which further radial localization is not operationally resolvable within the semiclassical description.

Null-ordered layering and holographic compression. As matter accumulates in the near-horizon region, extreme redshift organizes infalling degrees of freedom into a sequence of increasingly delayed null surfaces of approximately constant advanced

(or retarded) time. When the stretched-horizon scale is reached, this stratification naturally admits a description in terms of *null-ordered layers*, each associated with a distinct causal stage of collapse as viewed from infinity. In this regime, the horizon functions as an operational interface on which information about infalling matter may be encoded without reference to further radial structure.

Preserved lateral dynamics on the stretched horizon. While radial motion becomes arbitrarily suppressed in external time, tangential propagation remains fully active. For a null angular displacement at fixed radius r,

$$0 = -\Big(1 - \frac{r_s}{r}\Big)dt^2 + r^2 d\Omega^2, \tag{54}$$

which gives the coordinate angular velocity

$$\frac{d\Omega}{dt} = \frac{\sqrt{1 - r_s/r}}{r}. \tag{55}$$

The local proper time satisfies

$$d\tau_{\rm loc} = \sqrt{1 - \frac{r_s}{r}}\; dt, \tag{56}$$

so the locally measured angular rate is

$$\frac{d\Omega}{d\tau_{\rm loc}} = \frac{1}{r}. \tag{57}$$

The corresponding tangential speed is therefore

$$v_\perp = r\,\frac{d\Omega}{d\tau_{\rm loc}} = c. \tag{58}$$

Thus, even arbitrarily close to the horizon, null signals propagate laterally at the speed of light when measured with respect to local proper time, while radial motion is progressively frozen in the external description. This separation of suppressed radial dynamics and preserved tangential dynamics underlies the effective dimensional reduction of near-horizon physics and motivates the use of a horizon-based, null-ordered description.

3.6 Planck-Scale Horizon Dynamics and Causal Incorporation

As infalling matter becomes null-ordered within the near-horizon region, its information is incorporated into the horizon degrees of freedom through discrete *causal incorporation* events. These events are treated here as Planck-scale bookkeeping updates that register the completion of one unit of accumulated geometric mass at the stretched horizon. Each completed update increases the Schwarzschild radius by

$$\Delta r_s = 2\,\ell_{\rm p}, \tag{59}$$

and advances the internal causal ordering parameter by one step.

The update rule is purely kinematic: it does not assume microscopic mass quantization, nor does it specify the underlying dynamics by which infalling matter is processed. It serves only to define a consistent ordering of completed incorporations and an associated increment of horizon geometry.

Although the mass increment is Planck-scale, the corresponding area increment is macroscopic,

$$\Delta A = 16\pi r_s\, \ell_{\rm p}, \qquad \frac{\Delta A}{\ell_{\rm p}^2} = 32\pi \frac{m_{\rm bh}}{m_{\rm p}}, \tag{60}$$

so that for an astrophysical black hole a single completed update corresponds to an enormous increase in the number of available horizon degrees of freedom. Internal time $t_{\rm internal}$ is identified operationally with the count of such completed updates and is naturally associated with the proper-time parameter of the stretched horizon.

Global updating and causal consistency. A completed incorporation updates the geometric parameters of the horizon as a whole through the change of the mass parameter M. This update does not require the propagation of signals across the horizon surface. Rather, it reflects the fact that the null generators defining the horizon are globally determined by M, so that a change $M \to M + \Delta M$ induces a corresponding change in the location and area of the horizon in a single causal description. The use of an effective update map,

$$\Psi_{\mathcal{M}}(t_{n+1}) = \mathcal{U}_n\, \Psi_{\mathcal{M}}(t_n), \tag{61}$$

is therefore schematic and represents the coarse-grained redefinition of horizon data associated with a completed incorporation, not a literal unitary operation acting instantaneously on physical degrees of freedom.

Gravitational redshift ensures that one internal update corresponds to a very long interval of external Schwarzschild time,

$$t_{\rm ext} \sim (1 + z_{\rm h})\, t_{\rm p} \gg t_{\rm p}, \tag{62}$$

so that from infinity the same process appears arbitrarily slow, while from the internal bookkeeping perspective it advances in discrete steps. No violation of causality is implied.

Finite causal throughput and possible outflows. The combination

$$P_{\rm max} \equiv \frac{c^5}{G} \tag{63}$$

defines a characteristic Planck-scale causal rate that appears naturally in dimensional analyses of near-horizon physics. In the present framework this quantity is introduced only as a reference scale, not as a rigorously derived processing bound.

If, in a realistic astrophysical setting, infalling matter delivers energy and information faster than the horizon degrees of freedom can be incorporated into completed

updates, excess energy must be redistributed through channels that do not require further radial compression. Collimated outflows along pre-existing low-density or magnetically structured directions provide one plausible mechanism for such redistribution. In this sense, relativistic jets may be interpreted phenomenologically as a byproduct of finite near-horizon causal throughput, though no detailed jet dynamics are derived here.

Unified picture. Radial freezing, null ordering, preserved tangential propagation, discrete Planck-scale incorporation, and macroscopic horizon growth are all consequences of the same underlying structure: extreme gravitational redshift near the horizon combined with an information-limited reconstruction of geometry. Internal time advances only through completed incorporation events, while the external description stretches these events over arbitrarily long durations. The stretched horizon therefore functions as a radially frozen yet laterally active two-dimensional surface on which near-horizon physics may be consistently encoded.

3.7 Relativity of Planck Scales and Horizon-Defined Time

In a spacetime holographically reconstructed from the horizon of a parent black hole, the fundamental Planck quantities retain their standard local definitions. They do not vary dynamically and are not renormalized by position within a holographic hierarchy. Rather, they acquire a *relational interpretation* when physical processes are compared across distinct causal frames connected by strong gravitational redshift.

At every level of the hierarchy, locally defined Planck units are given by

$$m_{\rm p} = \sqrt{\frac{\hbar c}{G}}, \qquad \ell_{\rm p} = \sqrt{\frac{\hbar G}{c^3}}, \qquad t_{\rm p} = \frac{\ell_{\rm p}}{c}, \qquad E_{\rm p} = m_{\rm p} c^2. \tag{64}$$

Because the constants $\hbar$, c, and G are universal, these relations hold identically in every local proper frame, whether that frame belongs to an asymptotic exterior spacetime or to an emergent interior description.

Horizon-defined time and causal updates. In the horizon-layered framework, the physically relevant notion of time for the emergent interior is not an independent background parameter. Instead, internal time is identified with the ordered sequence of completed *causal incorporation events* on the horizon. Each such event corresponds to the incorporation of one geometric Planck-mass unit of information–energy into the horizon code and is associated with a single global retessellation of the horizon lattice.

The natural clock governing these updates is that of a static observer hovering at a proper distance $\ell_{\rm p}$ above the horizon. This observer experiences extreme gravitational redshift relative to infinity and may be identified operationally with the horizon itself, understood as a collective, stationary causal object. One Planck-time interval $t_{\rm p}$ measured by this near-horizon static observer defines one elementary "tick" of internal causal time.

If $N_{\rm inc}$ denotes the total number of completed Planck-mass incorporations, the internal time parameter is therefore

$$t_{\rm int} = N_{\rm inc}\, t_{\rm p}. \tag{65}$$

Internal time advances only when a new incorporation event occurs. When accretion proceeds steadily, these ticks occur in rapid succession from the interior perspective, generating a smoothly evolving cosmological time. When accretion slows or ceases, incorporation events become sparse or halt entirely, and internal time correspondingly slows or pauses.

Redshift and the invisibility of time halts. From the parent (asymptotic) frame, processes occurring arbitrarily close to the horizon are subject to enormous gravitational time dilation. The correspondence between parent coordinate time t and horizon-defined internal time $t_{\rm int}$ may be expressed schematically as

$$\frac{dt_{\rm int}}{dt} \sim \frac{1}{1+z_{\rm h}} \ll 1, \tag{66}$$

so that a single internal Planck-time tick corresponds, in the parent description, to a vastly longer external duration,

$$\Delta t_{\rm parent} \sim (1+z_{\rm h})\, t_{\rm p}. \tag{67}$$

This relation reflects gravitational redshift, not any modification of the Planck time itself.

Crucially, internal observers cannot detect periods during which incorporation halts or slows. All internal physical processes, clock rates, quantum phases, field evolution, and biological timescales, are reconstructed from the same sequence of horizon updates. When no updates occur, no internal process advances relative to any other. From the interior perspective, the distinction between continuous evolution and extremely sparse updates is operationally meaningless: time simply proceeds normally whenever it proceeds at all.

Energy scales and causal throughput. Because energy and time enter physical processes as conjugate variables, an external observer assigns proportionally redshifted energy scales to the same near-horizon events,

$$E_{\rm eff}^{(\rm parent)} \sim \frac{E_{\rm p}}{1+z_{\rm h}}, \tag{68}$$

even though the locally measured action scale remains unchanged. In particular, the ratio

$$\frac{E_{\rm p}}{t_{\rm p}} = \frac{c^5}{G} \tag{69}$$

serves as a universal dimensional benchmark linking energy, time, and gravity. It characterizes the maximal causal throughput of the horizon code and is invariant across all frames. It is not interpreted as a literal power or flux, but as a fundamental scale governing Planck-level causal updates.

Invariant entropy and horizon geometry. This relational interpretation ensures that the holographic entropy relation

$$S = \frac{A}{4\,\ell_{\mathrm{p}}^2} \tag{70}$$

holds identically for all horizons. Both the Planck area ℓ_{p}^2 and the information density per unit area are invariant. Gravitational redshift alters perceived rates and temporal ordering, not the information content of a fixed horizon configuration.

For a horizon of area A, the number of Planck-scale surface elements,

$$N = \frac{A}{\ell_{\mathrm{p}}^2}, \tag{71}$$

is therefore observer-independent. While N increases as the horizon grows through accretion, its value for any given configuration is the same in all causal frames. Observers disagree only on the external time separating successive horizon updates, not on the geometric or informational content of the horizon itself.

In this framework, temporal evolution is identified fundamentally with the ordered sequence of horizon incorporations. Planck scales are not variable constants but *relational markers* connecting locally invariant physics across strongly redshifted causal domains. Internal time is generated, paused, and resumed by the horizon's causal dynamics, yet remains experientially continuous for internal observers because all physical processes are synchronized to the same horizon-defined clock. This establishes a consistent notion of time across holographic hierarchies without introducing additional temporal structure beyond that supplied by the null-surface encoding itself.

3.8 Time as the Order of Horizon Code Configurations

In the horizon-layered framework, time is not introduced as a background parameter but emerges as an *ordering relation* on a sequence of globally defined horizon code configurations. Each configuration Σ_i represents a complete, self-consistent encoding of the horizon degrees of freedom after the i-th completed incorporation event at the stretched horizon. The passage of time is identified with the ordered succession of these configurations,

$$t_{\mathrm{internal}} \;\equiv\; \mathcal{O}(\{\Sigma_1, \Sigma_2, \Sigma_3, \dots\})\,, \tag{72}$$

where $\mathcal{O}$ denotes the causal ordering induced by completed incorporations of geometric mass at the horizon.

Each completed incorporation corresponds to the successful assimilation of one Planck unit of geometric mass into the horizon bookkeeping. Operationally, this event defines a single internal tick of duration t_{p}, not because microscopic dynamics proceed in discrete jumps, but because only completed incorporations generate a new, well-defined horizon configuration. Internal time therefore advances only when a new configuration Σ_{i+1} replaces Σ_i; unresolved micro-level processes do not contribute to the internal temporal ordering.

Each such update induces a global reorganization of the horizon code in the sense of a retessellation of degrees of freedom consistent with the new horizon area and mass parameter. This reorganization is local in the code variables and gauge-invariant, but it is global in its geometric meaning: the horizon is redefined as a new null surface with an updated Schwarzschild radius. In the reconstructed bulk description, the discreteness of these updates appears as coarse graining and gives rise to effective probabilistic behavior, reflecting limited information resolution rather than fundamental indeterminism.

From the external viewpoint, infalling matter approaches the horizon along null trajectories of approximately constant advanced time,

$$v = t + r_*, \qquad r_* = r + r_s \ln\left|\frac{r}{r_s} - 1\right|. \tag{73}$$

Successive completed incorporations correspond to successive increments of this advanced-time label. Accordingly, the internal ordering of horizon configurations may be put into correspondence with the external advanced-time sequence,

$$t_{\text{internal}} = N\, t_{\text{p}} \quad \longleftrightarrow \quad v = v_0 + N\, \delta v_{\text{p}}, \tag{74}$$

where N counts the number of *completed* Planck-mass incorporations and δv_{p} denotes the (generally large) advanced-time interval associated with one such completion as measured from infinity. This correspondence is kinematic and relational; no equality of clocks across frames is assumed.

Since each completed incorporation increases the black-hole mass by one Planck mass,

$$N = \frac{m_{\text{bh}}}{m_{\text{p}}}, \tag{75}$$

and using the identity

$$\frac{t_{\text{p}}}{m_{\text{p}}} = \frac{G}{c^3}, \tag{76}$$

the cumulative internal time associated with a horizon of mass m_{bh} may be written as

$$\boxed{t_{\text{internal}} = \frac{m_{\text{bh}} G}{c^3}} \tag{77}$$

in SI units. Equivalently, introducing the geometric mass $M_{\text{bh}} = G m_{\text{bh}}/c^2$, this bookkeeping relation becomes

$$\boxed{t_{\text{internal}} = \frac{M_{\text{bh}}}{c}.} \tag{78}$$

These expressions should be understood as definitions fixing the normalization of the internal time parameter, not as dynamical evolution laws.

Cessation and resumption of internal time. If accretion halts, the horizon mass remains constant and no new completed incorporations occur. The sequence of configurations $\{\Sigma_i\}$ therefore terminates temporarily, and internal time does not advance. The final configuration remains stationary and fully coherent. When accretion resumes, the next completed incorporation generates a new configuration Σ_{N+1}, and internal time resumes without memory or discontinuity. Internal observers experience continuous temporal flow because their physics is tied to the ordered sequence of configurations, not to the external duration between them.

Global updating without lateral signaling. Although no signal can propagate laterally across a macroscopic horizon within a single Planck interval, a horizon update is not a communication process on the surface. A null surface is defined globally by the mass parameter M: when $M \to M + \ell_{\mathrm{p}}$, the entire family of null generators is redefined geometrically. The update is therefore a global shift in the definition of the horizon, not the result of signals traversing it. Internal Planck ticks correspond to the redshifted proper-time intervals associated with these completed geometric updates, while externally the change appears as an asymptotically slow modification of the causal boundary.

In this framework, **each completed Planck-mass incorporation produces one global, horizon-wide causal reconfiguration**, and the ordered sequence of such reconfigurations $\{\Sigma_i\}$ constitutes the operational definition of cosmic time. Gravitational growth, entropy increase, and temporal ordering are thus unified as aspects of a single holographic bookkeeping structure, in which the history of horizon code updates *is* the time experienced by the reconstructed interior universe.

4 The Holographic Membrane

In the horizon-layered cosmology, the event horizon is treated not as a passive geometric boundary but as an active, null-synchronized membrane carrying Planck-scale degrees of freedom. From the external observer's perspective, infalling matter approaches the horizon only asymptotically in Schwarzschild time. Once gravitational redshift reaches the Planck regime, further radial evolution ceases to be operationally resolvable, and infalling matter is assimilated through *discrete completed incorporations* at the stretched horizon. Each completed incorporation corresponds to a Planck-scale increment in the geometric mass parameter, triggers a global retessellation of the membrane, and updates the adjacency relations of its constituent cells. The horizon therefore functions as a self-updating causal code, whose ordered sequence of configurations encodes the data from which the interior spacetime is reconstructed.

At the microscopic level, the membrane is modeled as a locally connected, approximately hexagonal adjacency graph, with each Planck-area cell having $\mathcal{O}(6)$ nearest neighbors. This near-hexagonal valence provides the discrete tangential directions that seed the two angular dimensions of the emergent bulk. The *generational index* associated with completed incorporations supplies the radial ordering, while the null ordering of successive global retessellations defines the internal time parameter. The (3+1)-dimensional interior geometry is therefore not assumed a priori but reconstructed incrementally from the horizon's two-dimensional causal structure. Horizon cells themselves do not propagate; rather, each global update reindexes the existing degrees of freedom and appends new cells carrying generational labels fixed by the cumulative horizon growth.

Localized excitations of the membrane encode all effective bulk matter and radiation. Stable, recurrent patterns of adjacency, phase, and causal accessibility correspond to particle species, while their apparent bulk motion arises from update and propagation rules defined on the membrane. Gravitational curvature is associated with local deficits or anisotropies in causal connectivity: regions where the effective lateral bandwidth of the membrane is reduced and neighboring links must be reconfigured. Such connectivity deficits project, in the coarse-grained description, to spacetime curvature in the reconstructed bulk, while uniform connectivity projects to flat geometry. In this sense, gravitation appears not as a fundamental bulk force but as the geometric consequence of maintaining holographic consistency on a finite, information-limited surface.

From an informational perspective, each Planck-scale link carries a finite set of causal states. Information is stored not in homogeneous configurations, fully connected or fully disconnected, but in the detailed pattern of allowed and disallowed connections across the membrane. Mass–energy corresponds to persistent, localized reductions in causal connectivity, while curvature reflects the collective redistribution of links required to accommodate such deficits. In the continuum limit, the familiar gravitational field equations arise as an effective bookkeeping description of how the membrane reallocates its finite causal and informational capacity.

These properties are not imposed ad hoc but follow from the structure of gravitational collapse. The event horizon must be a *closed* null surface: only compact surfaces can saturate the Bekenstein–Hawking entropy bound and serve as maximal information boundaries. A null surface with an edge would permit information leakage, render the holographic encoding non-invertible, and obstruct a consistent reconstruction of the interior. Accordingly, the spherical (or weakly deformed, e.g. Kerr) topology of the parent horizon is not a modeling choice but the generic end-state of collapse under causal and entropic constraints.

Completed incorporations must be globally well defined: each update corresponds to a single causal redefinition of the null surface. Such synchronization is possible only for compact horizons, where causal relations close consistently and lateral connectivity remains intact. Open or noncompact surfaces would disrupt global retessellation, compromise lateral propagation, and violate the algebraic and geometric constraints required for coherent entanglement structure in the emergent bulk.

The horizon processes information at an invariant causal throughput scale c^5/G, distributed across its degrees of freedom during each completed update. Uniform distribution of this causal flux requires a closed topology: open surfaces would accumulate or lose flux at their boundaries, breaking causal invariance. Only a compact null surface supports the null-ordered retessellation necessary to generate a coherent interior spacetime with Lorentzian causal structure.

4.1 Membrane Dipole Encoding

In this subsection we introduce a *phenomenological encoding model* for horizon microstructure, intended to provide a concrete realization of holographic boundary degrees of freedom and to explore possible consequences for emergent bulk composition. The construction is explicitly *model-level*: it is not claimed to represent fundamental microscopic physics, but rather an effective encoding scheme consistent with holographic bounds, causal constraints, and horizon thermodynamics.

The holographic membrane is modeled as a two-dimensional null surface coarse-grained into Planck-area cells. Each cell is endowed with two idealized *causal dipoles*: a *primary dipole* aligned with the local null normal of the horizon, and a *secondary dipole* oriented randomly. These dipoles are not assumed to be particles, fields, or geometric primitives; rather, they serve as minimal bookkeeping elements encoding causal connectivity, excision, and phase relations on the membrane.

Primary dipole: causal excision and gravitational charge. Each horizon-incorporated degree of freedom carries a primary dipole with one externally connected causal face and one inward-facing excised face. The excised orientation represents a localized withdrawal of causal connectivity, which in the emergent bulk description is associated with gravitational curvature. Spatial variations in the density and orientation of such excised faces encode, in the parent spacetime, the gravitational field, while in the horizon-layered internal description they label successive incorporation layers.

Secondary dipole: lateral coherence and matter sectors. The secondary dipole determines whether a given horizon degree of freedom can participate in coherent lateral causal networks. Only secondary dipoles whose orientation lies within a tangential acceptance cone of half-angle γ relative to the local horizon plane are permitted to establish lateral connectivity:

$$|\beta| < \gamma, \tag{79}$$

where β denotes the deviation from exact tangency. Degrees of freedom satisfying this condition may contribute to emergent matter or radiation sectors; those outside the cone remain non-propagating and vacuum-like in the bulk reconstruction.

Edge connectivity and dipole statistics. Each secondary dipole is assigned two lateral "edges", each of which may be connected with probability $(1-p)$ or disconnected with probability p. This yields the effective fractions

$$\begin{aligned} f_{\text{dark matter}} &= (\sin\gamma)\, p^2, \\ f_{\text{baryon}} &= (\sin\gamma)\, 2p(1-p), \\ f_{\text{massless}} &= (\sin\gamma)\, (1-p)^2, \\ f_{\text{vacuum}} &= 1 - \sin\gamma, \end{aligned} \tag{80}$$

which should be interpreted as *relative weights of emergent bulk sectors* rather than literal particle counts.

Choosing

$$\gamma = 18^\circ, \qquad p = \frac{11}{12}, \tag{81}$$

one obtains

$$f_{\text{baryon}} \simeq 0.048, \qquad f_{\text{dark matter}} \simeq 0.262, \qquad f_{\text{vacuum}} \simeq 0.691, \qquad f_{\text{massless}} \simeq 0.002,$$

in close numerical agreement with observed cosmological energy fractions. Within the present framework, this agreement is not claimed as a derivation, but as a *testable coincidence* suggesting that bulk composition may be encoded in horizon-level orientation statistics.

Geometric origin of orientation parameters. The angular tolerance γ and the discrete connectivity probabilities are motivated by the unavoidable topological constraints of spherical tilings. Any quasi-hexagonal tessellation of a closed surface requires twelve pentagonal defects; the associated icosahedral–dodecahedral dual structure provides a finite set of preferred tangential directions. In the present model, these directions define the allowed secondary-dipole orientations, linking horizon topology to bulk sector weights.

Propagation as pattern transfer, not cell motion. Horizon cells themselves are fixed bookkeeping sites. Apparent particle motion in the emergent bulk corresponds to the propagation of coherent secondary-dipole patterns across neighboring cells. An identity excitation is represented by a compact, phase-coherent configuration of secondary dipoles, whose envelope propagates by successive reassignment of orientations

on cells compatible with causal ordering. In this way, bulk trajectories arise from pattern drift on a static horizon lattice.

Massless, massive, and vacuum excitations. Purely tangential, fully connected secondary dipole configurations correspond to massless excitations propagating at the maximal lateral update rate. Mixed connectivity patterns produce massive, localized excitations, while strongly misaligned secondary dipoles fail to propagate coherently and contribute only to vacuum energy in the bulk description. Purely tangential, fully disconnected secondary dipole configurations correspond to dark matter excitations. Because they are causally disconnected, they can interact only gravitationally.

Recursive interpretation. If one adopts a parent–child universe interpretation, the same encoding rules may be applied recursively: primary dipoles of the parent horizon become tangential coherence carriers in the emergent interior, while secondary dipoles define radial ordering. This inversion preserves causal separation between generations while transmitting statistical encoding rules.

In summary, the membrane dipole encoding provides a concrete, if speculative, example of how bulk gravity, matter sectors, and vacuum energy might arise from simple causal bookkeeping rules on a null holographic surface. Its principal value lies not in microscopic literalism, but in the fact that a small set of geometric and probabilistic assumptions yields a nontrivial, falsifiable prediction for cosmic composition.

4.2 Hexagonal Horizon Geometry, Radial Indexing, and the Emergence of Three Spatial Dimensions

A nearly uniform quasi-hexagonal tessellation of the stretched horizon arises naturally as the configuration that maximizes local equidistance among Planck-scale degrees of freedom distributed on a compact two-dimensional surface. In two dimensions, hexagonal packing provides the densest and most isotropic arrangement of nearest neighbors, and any tension-regulated null membrane admitting local equilibration relaxes toward an approximately hexagonal adjacency structure.

A perfect hexagonal tiling, however, is incompatible with the topology of a closed sphere. Euler's theorem for polyhedral decompositions,

$$\chi = V - E + F, \qquad \chi_{\mathbb{S}^2} = 2,$$

implies that any lattice covering a spherical surface must contain a finite number of curvature defects. Since hexagons have internal angles of 120°, three meeting at a vertex produce zero Gaussian curvature. Positive curvature can only be supplied by polygons with smaller internal angles, namely pentagons. A standard application of Euler's theorem shows that *exactly twelve* pentagonal defects are required to close an otherwise hexagonal tiling on a sphere.

Accordingly, a Planck-thick stretched horizon is modeled as a quasi-hexagonal lattice containing twelve unavoidable pentagonal curvature defects. These defects act as topologically distinguished sites in the horizon adjacency graph and provide a discrete

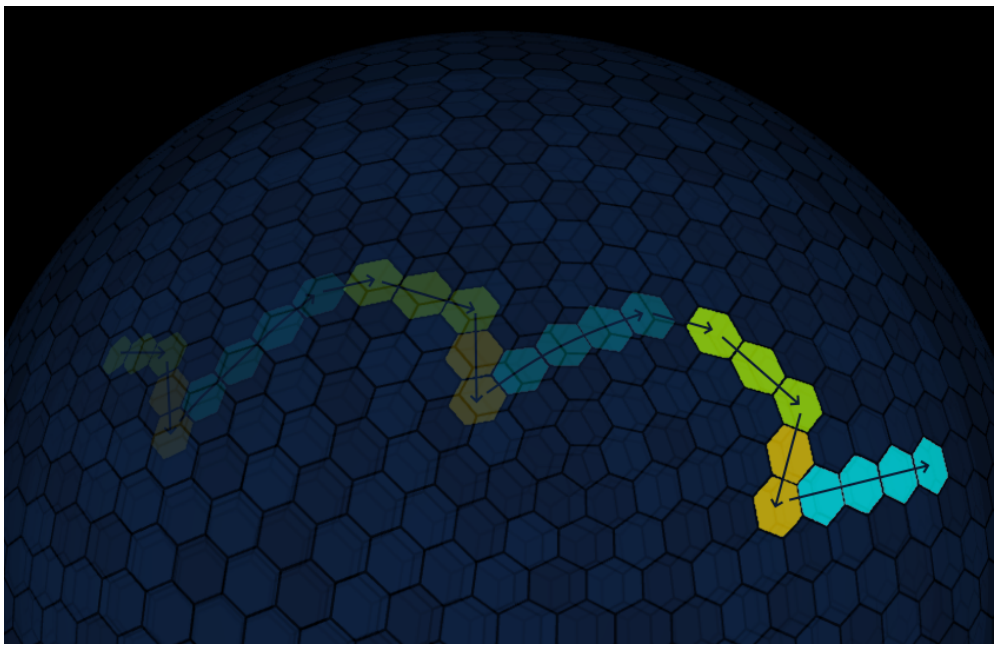

Fig. 4 Schematic representation of propagation along the event horizon. The depicted trajectory follows a fixed directional vector in the emergent three–dimensional bulk (e.g., $3x+2y+4z+1g$), while remaining confined to the two–dimensional null surface. Three successive generations of Planck–scale horizon shells are shown, each composed of quasi–hexagonal cells; together they illustrate how lateral propagation on the horizon is experienced internally as motion through emergent 3D space. Hexagonal sphere created by @arscan.

geometric scaffold that anchors large-scale anisotropies in the reconstructed interior. No microscopic dynamics are assumed in this argument; it is a purely topological consequence of compactness and local near-uniform connectivity.

Each horizon cell therefore has approximately six tangential neighbors, forming a locally six-valent causal lattice. These neighbors naturally group into three opposing pairs,

$$(\hat{e}_{+1}, \hat{e}_{-1}), \qquad (\hat{e}_{+2}, \hat{e}_{-2}), \qquad (\hat{e}_{+3}, \hat{e}_{-3}),$$

which define three independent tangential directions on the membrane. While these directions span only two angular dimensions intrinsically, their sixfold valence provides exactly three independent axes for lateral propagation in the coarse-grained description. These axes seed the three spatial directions of the reconstructed interior, but they do not by themselves define a radial dimension.

Radial indexing from horizon growth. The radial coordinate of the reconstructed interior is supplied not by membrane geometry but by the *generational ordering* of completed horizon updates. Each completed incorporation of one Planck unit of geometric mass increases the parent black hole mass from m_{bh} to $m_{\mathrm{bh}}+m_{\mathrm{p}}$ and advances

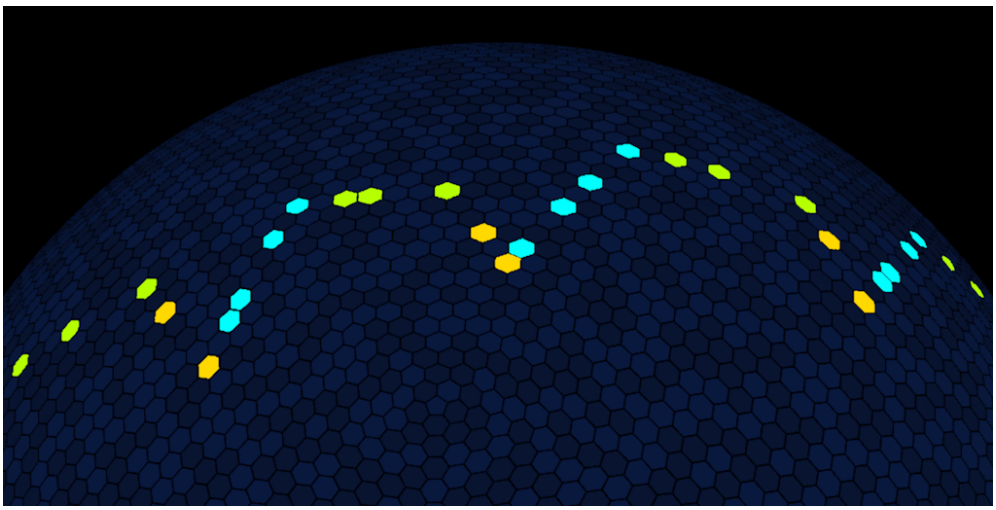

Fig. 5 Schematic representation of how propagation on a hexagonally tessellated horizon is actually realized. A signal following an effective bulk direction (e.g. $3x + 2y + 4z + 1g$) moves only between neighboring Planck cells, and each hop is constrained by the local generational rule: transitions into cells with $g_{\rm cell} \leq g_{\rm signal}$ are allowed, while neighbors with $g_{\rm cell} > g_{\rm signal}$ are forbidden. Propagation is therefore implemented as a strictly local adjacency filter that preserves radial generational ordering without any nonlocal search. Hexagonal sphere created by @arscan.

the Schwarzschild radius

$$r_{\rm s} = \frac{2Gm_{\rm bh}}{c^2}. \tag{82}$$

The horizon area

$$A = 4\pi r_{\rm s}^2 \tag{83}$$

therefore increases by

$$\Delta A \simeq 8\pi r_{\rm s}\,\Delta r_{\rm s}, \tag{84}$$

so that each completed update adds

$$\Delta N_{\rm cell} = \frac{\Delta A}{\ell_{\rm p}^2} \simeq 32\pi\,\frac{m_{\rm bh}}{m_{\rm p}} \tag{85}$$

new Planck-area cells to the stretched horizon.

Because each update corresponds to the same mass increment $\Delta m = m_{\rm p}$, the effective mass-per-cell associated with a given generation is

$$\mu_g \equiv \frac{\Delta m}{\Delta N_{\rm cell}} \simeq \frac{m_{\rm p}^2}{32\pi\, m_{\rm bh}(g)}, \tag{86}$$

which decreases monotonically as the horizon grows. This quantity is recorded as a *primary-dipole weight* attached to each cell created in that update. In this sense, every horizon cell carries a fixed generational label $g_{\rm cell}$ encoding the cumulative horizon

mass at the time of its creation. This label functions as a holographic proxy for radial position in the reconstructed interior.

Generational filtering and locality. An excitation created at incorporation step $g_{\rm inc}$ is assigned a signal index

$$g_{\rm signal} = g_{\rm inc}. \tag{87}$$

Local propagation on the membrane is subject to the generational accessibility rule

$$g_{\rm cell} \leq g_{\rm signal}, \tag{88}$$

which is checked only against nearest neighbors at each null step. Moves toward cells with larger generational index are forbidden. This rule enforces radial ordering without requiring nonlocal searches or global knowledge of the horizon state. Because successive retessellations interleave generations locally, every cell retains accessible neighbors, and propagation remains strictly local and causal.

Tangential propagation and coarse-grained motion. A signal propagates laterally via sequences of null steps,

$$W = \hat{e}_{i_1}\hat{e}_{i_2}\cdots\hat{e}_{i_N}. \tag{89}$$

The coarse-grained displacement along the three tangential axes is

$$(\Delta_1, \Delta_2, \Delta_3) = (N_{+1} - N_{-1},\, N_{+2} - N_{-2},\, N_{+3} - N_{-3}), \tag{90}$$

which determines the angular component of the reconstructed bulk trajectory. Multiple null-step sequences correspond to the same coarse displacement, giving rise to wave-like interference patterns in the effective interior description.

Expansion as signal renormalization. The stretched-horizon radius increases discretely,

$$r_{\rm s}(t+1) = r_{\rm s}(t) + 2\ell_{\rm p}, \tag{91}$$

but horizon cells retain their fixed generational labels and primary-dipole weights. To preserve homogeneity and isotropy in the reconstructed interior, comoving excitations must drift outward even in the absence of dynamical radial motion. This is implemented by a global rescaling of the *signal index* alone,

$$g_{\rm signal}(t+1) = \lambda(t)\, g_{\rm signal}(t) + \delta g, \qquad \lambda(t) = 1 + \frac{2\ell_{\rm p}}{r_{\rm s}(t)}, \tag{92}$$

where δg represents genuine interaction-induced radial motion. No membrane cell moves; only the interpretation of signal indices changes under successive updates.

Information-limited radial reconstruction. The generational index g is not a Schwarzschild radial coordinate but a null-ordered causal label recording the sequence of completed horizon updates. When mapped into the reconstructed interior via the embedding map E_t, successive values of g correspond to successive radial shells whose

spacing is fixed not by external geometry but by the information-limited stacking of completed incorporations.

Each completed internal update contributes an equal increment of enclosed geometric mass, $\Delta M = \ell_{\mathrm{p}}$. Homogeneity of the reconstructed interior therefore requires that equal mass increments be assigned equal increments of enclosed interior volume in the coarse-grained description. This condition uniquely fixes the radial scaling.

Homogeneity requirement.

Let

$$M(g) = \ell_{\mathrm{p}}\, g \tag{93}$$

denote the enclosed geometric mass associated with completed update index g. Homogeneity at fixed internal time requires

$$M(g) \propto V_{\mathrm{enc}}(g) \propto r_{\mathrm{phys}}(g)^3, \tag{94}$$

so that the coarse-grained density

$$\rho = \frac{M(g)}{\frac{4\pi}{3}\, r_{\mathrm{phys}}(g)^3} \tag{95}$$

is independent of radius. Consequently,

$$r_{\mathrm{phys}}(g) \propto g^{1/3}. \tag{96}$$

Stacking coordinate as a cumulative depth label.

We define a dimensionless comoving stacking coordinate $\chi(g)$ as a monotone cumulative depth label constructed from completed horizon updates,

$$\chi(g) \equiv \sum_{j=1}^{g} \Delta\chi(j), \qquad \chi(0) \equiv 0. \tag{97}$$

At this stage χ is defined only up to an overall normalization, which is fixed later by an operational choice once the scale factor $a(t)$ is introduced.

Scaling of $\Delta\chi(g)$.

Since χ is a comoving coordinate whose physical realization is given by $r_{\mathrm{phys}}(g) = a(t)\,\chi(g)$, the scaling

$$\chi(g) \propto g^{1/3} \tag{98}$$

is required by homogeneity. In the large-g continuum approximation, $\Delta\chi(g) \sim d\chi/dg$, this implies

$$\Delta\chi(g) \propto g^{-2/3}. \tag{99}$$

Early generations therefore correspond to large comoving radial increments, while later generations correspond to increasingly fine increments. This information-geometric scaling smooths the reconstructed radial direction and eliminates the appearance of a central density divergence.

In this reconstruction, the full three-dimensional bulk emerges as follows: quasi-hexagonal adjacency supplies three tangential directions; generational indexing supplies radial ordering; generational filtering enforces locality; and signal renormalization under horizon growth produces comoving expansion. The horizon remains a fixed historical record of completed incorporations, while the interior geometry is the continually updated continuum interpretation of this null-ordered boundary data.

4.3 Hubble Expansion, Scale Factor Dynamics, and FLRW Correspondence

In the horizon-layered cosmology, the expansion of the emergent interior spacetime is a direct consequence of the discrete, null-ordered growth of the parent black-hole horizon. Each completed incorporation of one Planck unit of geometric mass advances the internal causal order by one tick and increases the Schwarzschild radius by a fixed Planck-scale increment,

$$r_{\mathrm{s}}(t + t_{\mathrm{p}}) = r_{\mathrm{s}}(t) + 2\ell_{\mathrm{p}}. \tag{100}$$

To maintain homogeneity and isotropy in the reconstructed interior, the radial index carried by every internal excitation must be rescaled by the same *fractional* amount under each completed horizon update. Denoting the generational label of a propagating excitation by g_{signal}, we write

$$g_{\mathrm{signal}}(t + t_{\mathrm{p}}) = g_{\mathrm{signal}}(t)\left(1 + \frac{2\ell_{\mathrm{p}}}{r_{\mathrm{s}}(t)}\right) + \delta g, \tag{101}$$

where δg represents genuine dynamical radial motion arising from local interactions. Neglecting δg isolates the pure background expansion.

Since physical bulk distances are reconstructed from the generational index via the scale factor, this update induces a proportional rescaling of all comoving radii,

$$r(t + t_{\mathrm{p}}) = r(t)\left(1 + \frac{2\ell_{\mathrm{p}}}{r_{\mathrm{s}}(t)}\right). \tag{102}$$

Defining the discrete expansion factor

$$\lambda(t) \equiv \frac{r(t + t_{\mathrm{p}})}{r(t)} = 1 + \frac{2\ell_{\mathrm{p}}}{r_{\mathrm{s}}(t)}, \tag{103}$$

and passing to the continuum limit yields

$$\frac{\dot{r}}{r} = \frac{\lambda(t) - 1}{t_{\mathrm{p}}} = \frac{2\ell_{\mathrm{p}}}{r_{\mathrm{s}}(t)}\,\frac{1}{t_{\mathrm{p}}}. \tag{104}$$

Using $\ell_{\mathrm{p}}/t_{\mathrm{p}} = c$, the effective expansion rate becomes

$$\boxed{H(t) \equiv \frac{\dot{r}}{r} = \frac{2c}{r_{\mathrm{s}}(t)}.} \tag{105}$$

Because all internal comoving separations scale in the same manner, the scale factor of the reconstructed FLRW interior satisfies

$$\frac{\dot{a}}{a} = H(t) = \frac{2c}{r_{\rm s}(t)}. \tag{106}$$

Using

$$r_{\rm s}(t) = \frac{2Gm(t)}{c^2}, \tag{107}$$

with the horizon mass growing monotonically as

$$m(t) = m_0 + \frac{m_{\rm p}}{t_{\rm p}}\, t, \tag{108}$$

one obtains

$$H(t) = \frac{c^3}{G\, m(t)}. \tag{109}$$

Integration then gives

$$a(t) = a_0 \exp\!\left(\int^t \frac{c^3}{G\, m(t')}\, dt' \right). \tag{110}$$

For linear mass growth, this reduces to

$$a(t) = a_0 \left(m_0 + \frac{m_{\rm p}}{t_{\rm p}}\, t \right), \tag{111}$$

so that the scale factor is proportional to the horizon mass. The expansion of the interior universe therefore tracks directly the discrete growth history of the enclosing horizon.

Proper distances obey the standard FLRW relation

$$d_{\rm phys}(t) = a(t)\, d_{\rm com}, \qquad H(t) = \frac{\dot{a}}{a}. \tag{112}$$

Thus the defining kinematic feature of FLRW cosmology—recession velocity proportional to separation—emerges directly from horizon-side causal ordering, without postulating bulk field equations or an equation of state.

The effective interior density is

$$\rho(t) = \frac{m(t)}{\frac{4\pi}{3} r_{\rm s}(t)^3} = \frac{3c^6}{32\pi G^3 m(t)^2}, \tag{113}$$

so that

$$\rho(t) \propto a(t)^{-2}. \tag{114}$$

This scaling differs from that of dust because the interior volume grows as $r_{\rm s}^3$ while the incorporated mass increases linearly. The resulting effective fluid behavior is fixed kinematically by holographic growth, not by microscopic matter dynamics.

Substituting these relations into the Friedmann equation,

$$H^2 = \frac{8\pi G}{3}\rho - \frac{k}{a^2}, \tag{115}$$

yields

$$H^2 = \frac{8\pi G}{3}\rho, \qquad \Rightarrow \qquad k = 0. \tag{116}$$

Spatial flatness is therefore selected uniquely by the area–volume relation implicit in the horizon reconstruction.

Isotropy and the generational index. Although the Schwarzschild radius increases in discrete steps $\Delta r_{\rm s} = 2\ell_{\rm p}$, this does not discretize or anisotropize bulk distances. The generational index g is a null-ordered causal label, not a geometric thickness. Because each generation corresponds to a complete spherical layer, the reconstructed radial coordinate is isotropic by construction. Bulk lengths are set by $a(t)$, not by the external Schwarzschild increments, and the interior remains locally Minkowskian.

Causal depth and the Hubble radius. In this framework the Hubble radius

$$r_{\rm h} \equiv \frac{c}{H} \tag{117}$$

is not a particle horizon but a causal-synchronization scale. Using $H(t) = 2c/r_{\rm s}(t)$ gives the exact identity

$$\boxed{r_{\rm h} = \frac{r_{\rm s}}{2},} \tag{118}$$

valid at all epochs. The observable universe therefore contains approximately half of the total encoded interior mass, not because of a geometric cutoff, but because only half of the null-ordered horizon incorporations have completed relative to the current internal time.

Unified picture. Discrete Planck-scale incorporation drives horizon growth; isotropy enforces a global rescaling of radial indices; and the resulting kinematics yield

$$a(t) \propto t, \qquad H(t) = \frac{1}{t}, \qquad k = 0. \tag{119}$$

The emergent interior is therefore a spatially flat, coasting FLRW universe whose expansion, density evolution, and observable causal depth arise entirely from the null-ordered growth of the holographic horizon.

4.4 Generational Mass Index, Horizon Discreteness, and the Emergence of a Smooth FRW Interior

A central structural insight of the horizon-layered cosmology is that the radial dimension of the emergent bulk does not pre-exist the horizon but is *constructed* from

its growth history. Each completed Planck-scale incorporation increases the geometric mass parameter of the black hole by $\Delta M = \ell_{\mathrm{p}}$ and therefore increases the Schwarzschild radius by the fixed increment

$$\Delta r_{\mathrm{s}} = \frac{2G\,\Delta m}{c^2} = 2\ell_{\mathrm{p}}. \tag{120}$$

Externally, the horizon thus grows through a strictly uniform sequence of radial updates. The corresponding area increment,

$$\Delta A = 8\pi r_{\mathrm{s}}\,\Delta r_{\mathrm{s}} = 16\pi r_{\mathrm{s}}\,\ell_{\mathrm{p}}, \tag{121}$$

creates

$$\Delta N_{\mathrm{cell}} = \frac{\Delta A}{\ell_{\mathrm{p}}^2} = \frac{16\pi r_{\mathrm{s}}}{\ell_{\mathrm{p}}} \tag{122}$$

new Planck-area cells on the stretched horizon, each endowed with an inward-facing *primary dipole*.

Because the incorporated mass $\Delta m = m_{\mathrm{p}}$ is fixed at each completed update, the effective mass-per-cell associated with the newly created generation is

$$\mu_g \equiv \frac{\Delta m}{\Delta N_{\mathrm{cell}}} = \frac{m_{\mathrm{p}}^2}{16\pi\, m_{\mathrm{bh}}(g)}, \tag{123}$$

which decreases monotonically as the total black-hole mass grows. This value is permanently inscribed in the primary dipole and functions as the cell's *generational label* g_{cell}.

Local propagation rules enforce the constraint

$$g_{\mathrm{cell}} \le g_{\mathrm{signal}},$$

so that each bulk excitation can access only those horizon cells whose mass-per-cell does not exceed its own. In this way the internal radial direction is defined informationally, as a cumulative ordering of decreasing μ_g, not as the Schwarzschild areal radius itself.

Information-weighted internal radial increments. Although the external horizon grows in uniform steps of $2\ell_{\mathrm{p}}$, the internal radial reconstruction cannot assign equal bulk thickness to each generation. Homogeneity of the reconstructed interior requires that equal mass increments correspond to equal increments of enclosed interior volume. This uniquely fixes the scaling of the comoving radial increments.

Let g denote the completed-update index, so that the enclosed geometric mass satisfies $M(g) = \ell_{\mathrm{p}} g$. Homogeneity then requires

$$M(g) \propto V_{\mathrm{enc}}(g) \propto r_{\mathrm{phys}}(g)^3, \tag{124}$$

which implies

$$r_{\mathrm{phys}}(g) \propto g^{1/3}. \tag{125}$$

Introducing a dimensionless comoving stacking coordinate $\chi(g)$, the continuum approximation $\Delta\chi(g) \sim d\chi/dg$ yields

$$\Delta\chi(g) \propto g^{-2/3}. \tag{126}$$

This scaling may equivalently be expressed in terms of horizon information capacity. A horizon layer at generation g has area

$$A_g = 4\pi r_{\rm s}(g)^2, \qquad N_{\rm cell}(g) = \frac{A_g}{\ell_{\rm p}^2},$$

so that the information-limited radial resolution scales as

$$\Delta\chi(g) \sim \frac{1}{N_{\rm cell}(g)} \propto \frac{\ell_{\rm p}^2}{r_{\rm s}(g)^2}. \tag{127}$$

Up to an overall normalization absorbed into the scale factor $a(t)$, this is precisely the scaling required by homogeneity.

The physical bulk radial increment contributed by generation g is therefore

$$\Delta r_{\rm bulk}(g) = a(t)\,\Delta\chi(g), \tag{128}$$

and the reconstructed interior radius is

$$r_{\rm bulk}(g) = a(t) \sum_{g'=1}^{g} \Delta\chi(g'). \tag{129}$$

Because $\Delta\chi(g')$ decreases monotonically, late generations contribute arbitrarily fine radial increments, while early generations contribute coarse ones. The resulting radial coordinate is continuous in the large-g limit.

Why the interior is smooth and isotropic. Although the horizon grows through discrete Planck-scale updates, their internal images are smoothed by information-weighted stacking. The scaling

$$\Delta r_{\rm bulk}(g) \propto g^{-2/3}$$

ensures that the sum over many generations converges to a differentiable radial coordinate. Uniform multiplication by the scale factor $a(t)$ enforces isotropy, so that no direction is distinguished in the reconstructed bulk.

The embedding map E_t interprets horizon steps $(\Delta_x, \Delta_y, \Delta_z, \Delta g)$ as bulk displacements according to the FLRW line element,

$$ds^2 = -dt^2 + a(t)^2\big(d\chi^2 + \chi^2 d\Omega^2\big)\,.$$

Tangential directions arise from six-valent hexagonal adjacency, while the radial direction arises from generational ordering; yet after embedding they are scaled uniformly

by $a(t)$ and become geometrically indistinguishable. No local bulk experiment can detect the discreteness of the horizon layering.

Discrete horizon, continuous bulk. Fundamental discreteness resides only on the horizon, which is tiled by Planck-area cells carrying primary and secondary dipoles. Bulk fields correspond to coarse-grained superpositions over enormous numbers of horizon cells; no bulk degree of freedom is supported on a single cell. As a result, the interior spacetime exhibits no lattice artifacts or preferred scales, and classical general relativity emerges as the continuum limit of horizon-side null dynamics.

Planck scales enter bulk physics only indirectly: the Planck time sets the retessellation cadence; the Planck area fixes the maximal causal throughput c^5/G; and $\hbar$ and G appear as renormalized parameters governing the effective algebra of coarse-grained phase excitations.

Interpretation of the embedding map. The embedding map E_t is not an additional dynamical structure imposed on the horizon. It is the unique information-theoretic reconstruction that internal observers must adopt in order to describe null-surface dynamics as a smooth, local, isotropic spacetime. Individual horizon cells carry no geometric data; geometry emerges only after coarse-graining many null interactions into a continuum correlation structure.

Conclusion. The generational mass index g is the holographic origin of the radial dimension. Decreasing μ_g defines causal depth, while information-weighted increments $\Delta\chi(g)$ convert discrete horizon layers into a continuous radial coordinate. Through the embedding map, Planck-scale discreteness on the horizon gives rise to a smooth, homogeneous, isotropic FRW interior. The internal geometry is therefore not assumed but reconstructed, arising inevitably from the causal stacking of horizon layers.

4.5 Emergence of Classicality from Bandwidth-Limited Coherence

A distinctive feature of the horizon-layered framework is that the quantum–classical transition arises not from environmental noise or ad hoc coarse-graining but from the *finite causal bandwidth* of the horizon. Each Planck-mass incorporation triggers a global, null-synchronized retessellation of the membrane, during which all secondary-dipole field configurations must be updated in a manner consistent with local adjacency relations and global algebraic constraints. The horizon's total causal throughput is bounded by

$$P_{\max} \sim \frac{c^5}{G},$$

so within each Planck interval t_{p} only a finite amount of phase and correlation information can be coherently maintained across the membrane. As systems become macroscopic and their field envelopes extend over enormous numbers of cells, sustaining a fully coherent superposition would require tracking an astronomically large set of relative phases within a single update, exceeding this global causal budget.

Consequently, high-complexity superpositions are dynamically fragile. As an apparatus and its environment couple to a system, the null-walk ensembles associated with different outcome sectors $\mathcal{S}_k$ diverge in horizon configuration space and rapidly lose

combinatorial overlap: their detailed phase relationships cannot all be preserved within the fixed throughput c^5/G. This produces *bandwidth-driven decoherence*: branches remain formally admissible within the kinematic Hilbert space, but only a restricted subset of sectors can be kept globally phase-consistent across successive retessellations.

At each subsequent global update, the horizon algebra stabilizes a single sector $\mathcal{S}_k$ whose dipole configurations, adjacency relations, and representation constraints are mutually consistent under the available causal bandwidth. All other sectors contain latent inconsistencies somewhere on the membrane and are therefore not sustained under further updates. To internal observers this appears as a stochastic wavefunction collapse; in the boundary description it is a deterministic consistency projection enforced by the finite causal throughput of a null-synchronized code.

Classicality then emerges as a robustness condition. Macroscopic configurations are precisely those coarse-grained dipole-phase patterns that can survive repeated global updates under the fixed causal budget c^5/G. Superpositions of such configurations are unstable because they demand more coherent phase tracking than the horizon can supply. The quantum–classical transition is thus an intrinsic property of the holographic code: decoherence and effective collapse follow from bandwidth-limited retessellation, without the need for an independent collapse postulate.

A subtle but essential feature of the horizon-layered framework is that, although the membrane permits lateral propagation only along six discrete hexagonal directions, the emergent bulk nevertheless exhibits an isotropic light cone with invariant speed c in the continuum limit. This arises because physical signals are not literal single-step hops on the lattice but extended null-wave ensembles: a photon corresponds to a superposition of all allowed null-walk sequences across the hexagonal adjacency graph. While each microscopic path is zig–zag and directionally anisotropic, the ensemble of all paths is rotationally symmetric at large scales, just as discrete lattices in relativistic field theory recover isotropic wave equations despite having only finitely many allowed move directions.

The embedding map E_t amplifies this symmetry by interpreting the coarse-grained displacement field generated by these null-step ensembles as a smooth bulk displacement. The resulting effective geometry is the unique isotropic metric compatible with the membrane's symmetry group,

$$ds^2 = -c^2dt^2 + a(t)^2\left(dr^2 + r^2d\Omega^2\right).$$

Thus the emergent speed of light is direction-independent in the bulk, even though microscopic propagation on the horizon is highly anisotropic.

This mechanism also explains why space and time appear fundamentally unified in the emergent interior. Null-step propagation on the horizon couples lateral adjacency (spatial displacement) with the fixed tick of causal retessellation (temporal advance), so the embedding map reconstructs a Lorentzian spacetime structure from purely two-dimensional null dynamics. The inseparability of space and time in the bulk is therefore not fundamental but emergent: it is the continuum projection of the membrane's bandwidth-limited, null-synchronized dynamics, which enforce an effectively

unified spacetime geometry even though the underlying causal processes treat lateral propagation and horizon-time updates as distinct operations.

4.6 Relativistic Kinematics from Causal Bandwidth and Field–Identity Separation

In the horizon-layered cosmology, relativistic effects arise from the finite causal throughput of the holographic horizon. Each Planck-scale cell can update its secondary-dipole (phase and correlation) data only at an invariant maximal rate,

$$\dot{\mathcal{I}}_{\max} = \frac{1}{t_{\mathrm{p}}} = \sqrt{\frac{c^5}{\hbar G}}, \tag{130}$$

which characterizes the fundamental update rate of the null-synchronized membrane. This finite causal budget must be allocated among three tasks: (i) maintaining the coherence of identity codewords, (ii) propagating field correlations laterally, and (iii) participating in global retessellation events. All relativistic kinematic effects arise from how this fixed causal budget is partitioned.

Primary vs. secondary dipoles. Primary dipoles are fixed, non-propagating properties of stationary horizon cells. They encode the cell's generational (radial) index and its causal excision weight. *Secondary dipole configurations*, by contrast, are the propagating data structures that carry all field, phase, and identity information. Bulk motion arises entirely from the migration of secondary-dipole patterns across the static primary-dipole lattice.

Massive particles: identity-bearing excitations. A massive particle corresponds to a compact, coherently organized cluster of secondary dipoles (an identity codeword $\mathcal{C}$) together with its surrounding field envelope $F_{\mathcal{C}}$. The secondary-dipole pattern associated with the identity migrates across neighboring horizon cells subject to the generational filter $g_{\mathrm{cell}} \leq g_{\mathrm{sig}}$. The codeword's effective worldline is given by the centroid of its propagating field pattern,

$$\mathcal{C}(t+1) = \mathrm{centroid}[F_{\mathcal{C}}(t+1)]. \tag{131}$$

However, a nonzero fraction of the local causal bandwidth must always be reserved to maintain the coherence of the identity pattern itself. This bandwidth cost enforces a sub-null drift: massive particles cannot propagate at the full lateral update rate c.

Massless particles: pure field propagation. A photon corresponds to a propagating secondary-dipole phase pattern without an identity core. Because no bandwidth is required for internal identity maintenance, essentially all available causal throughput can be devoted to lateral propagation along the six primitive null directions of the hexagonal lattice. The pattern therefore advances one Planck cell per Planck time and maps, under the embedding E_t, to a null trajectory in the emergent bulk,

$$|\dot{\gamma}(t)| = c. \tag{132}$$

Bandwidth allocation and time dilation. Let $\dot{\mathcal{I}}_{\mathrm{lat}}$ denote the bandwidth devoted to lateral propagation and $\dot{\mathcal{I}}_{\mathrm{int}}$ the bandwidth devoted to identity maintenance, with

$$\dot{\mathcal{I}}_{\mathrm{lat}} + \dot{\mathcal{I}}_{\mathrm{int}} = \dot{\mathcal{I}}_{\max}. \tag{133}$$

For an excitation whose effective bulk velocity is v, maintaining directional coherence of the field envelope requires allocating a fraction v/c of the available causal throughput to lateral propagation. The remaining bandwidth available for internal updates therefore scales as

$$\dot{\mathcal{I}}_{\mathrm{int}} = \dot{\mathcal{I}}_{\max}\sqrt{1 - v^2/c^2}. \tag{134}$$

The rate at which proper time accumulates along the excitation's worldline is then

$$\frac{d\tau}{dt} = \sqrt{1 - v^2/c^2}, \tag{135}$$

recovering the standard relativistic time-dilation relation. The associated relativistic energy takes the familiar form

$$E = \frac{m_0 c^2}{\sqrt{1 - v^2/c^2}}, \tag{136}$$

as a consequence of the same bandwidth reallocation.

Why massive trajectories are timelike. Because identity-bearing excitations must preserve internal coherence, they must allocate a nonzero share of the causal budget to $\dot{\mathcal{I}}_{\mathrm{int}}$. This necessarily limits the bandwidth available for lateral propagation and forces their effective drift velocity to satisfy $v < c$. Timelike geodesics thus emerge from the requirement that identity codewords maintain structural integrity across successive horizon updates.

Why massless trajectories are null. Massless excitations possess no identity core and therefore incur no internal coherence cost,

$$\dot{\mathcal{I}}_{\mathrm{int}} = 0, \qquad \dot{\mathcal{I}}_{\mathrm{lat}} = \dot{\mathcal{I}}_{\max}. \tag{137}$$

They may therefore saturate the lateral propagation channel and follow null geodesics in the emergent spacetime.

Inertia as resistance to identity deformation. Accelerating a massive excitation requires increasing the directional coherence of its propagating field pattern, which diverts bandwidth away from internal identity maintenance. The resistance of the identity core to this reallocation manifests as inertia: the cost, in causal throughput, of deforming a stable identity codeword.

Stress–energy as coarse-grained bandwidth flow. Spatial variations in how the membrane allocates causal bandwidth across its surface coarse-grain into the stress–energy tensor of the emergent bulk. Regions where lateral causal flow is systematically impeded (for example by strong secondary-dipole gradients or excision density) project

as curvature in the reconstructed spacetime. In this sense, the Einstein equations appear as a macroscopic bookkeeping relation governing the redistribution of causal bandwidth,

$$G_{\mu\nu} = \frac{8\pi G}{c^4} T_{\mu\nu}. \tag{138}$$

In this unified picture, massive and massless motion differ only in how they utilize the finite causal bandwidth of the horizon. Massive trajectories arise from propagating secondary-dipole patterns constrained by identity coherence, while massless trajectories arise from unconstrained lateral propagation. Time dilation, inertia, relativistic energy, and the distinction between timelike and null geodesics all emerge from a single organizing principle: the causal economics governing how the holographic membrane allocates its invariant throughput c^5/G.

4.7 Mach's Principle and the Origin of Inertia

In classical mechanics, inertia quantifies a system's resistance to changes in motion. Its origin has remained conceptually opaque: in Newtonian theory it is intrinsic; in Mach's view it is relational; and in general relativity it emerges from spacetime geometry shaped by global energy–momentum distributions.

In the horizon-layered cosmology, inertia appears as an explicit informational property of the holographic membrane. Each Planck cell participates in a null-synchronized causal lattice supporting both geometric adjacency and algebraic phase constraints. A massive excitation corresponds not to a fixed location on this lattice but to a *propagating secondary-dipole pattern*: a stable cluster of phase correlations that migrates laterally across horizon cells according to the membrane's update rules. The primary dipoles remain fixed and encode generational index (radial position), while the secondary dipoles carry identity and field information and are responsible for particle motion in the emergent bulk.

To accelerate a particle is therefore to modify the directional coherence of this propagating secondary-dipole pattern. Such a modification requires a reallocation of the finite causal bandwidth available to the local horizon region: more throughput must be devoted to maintaining directed lateral propagation, leaving less capacity available for internal identity maintenance. Acceleration is resisted because it demands a redistribution of coherence across the membrane's causal network.

This provides an operational realization of Mach's principle: **inertia is relational rather than intrinsic**. The effective inertial state of a particle corresponds to a configuration in which its secondary-dipole pattern maintains a stationary, statistically isotropic relationship with the surrounding horizon cells. Attempts to accelerate the particle disturb this relational equilibrium and require compensating adjustments in the surrounding causal structure. Because the horizon functions as a globally constrained system, the inertial response of any local excitation implicitly depends on the state of the larger causal network.

Formally, the effective inertial mass m_{eff} may be characterized heuristically as proportional to the rate at which the horizon code must adjust the mutual information between a local subsystem $\mathcal{S}$ and its complement $\bar{\mathcal{S}}$ in order to accommodate

acceleration,

$$m_{\text{eff}}c^2 \;\propto\; \frac{\partial I(\mathcal{S}:\bar{\mathcal{S}})}{\partial \tau}. \tag{139}$$

Uniform motion corresponds to a stationary mutual-information profile under successive retessellations, whereas acceleration requires a change in this profile, representing the informational work needed to reconfigure causal coherence. This reconfiguration consumes finite causal bandwidth and manifests macroscopically as inertia.

Within this framework, the equivalence principle follows naturally at the kinematic level. Gravitational mass and inertial mass coincide because both quantify the resistance of the null-synchronized causal network to changes in relational structure. Gravitational curvature describes how global connectivity redirects null propagation; inertia measures the bandwidth cost of modifying that propagation locally. Both arise from the same finite-capacity causal substrate.

In summary, within the horizon-layered cosmology, Mach's principle is realized operationally: **inertia reflects the relational resistance of the holographic membrane to reconfiguring its causal entanglement structure**. Local inertial frames are not primitive geometric entities but stable global connectivity patterns on the horizon. Motion, inertia, and gravitation emerge as interconnected aspects of a single informational architecture.

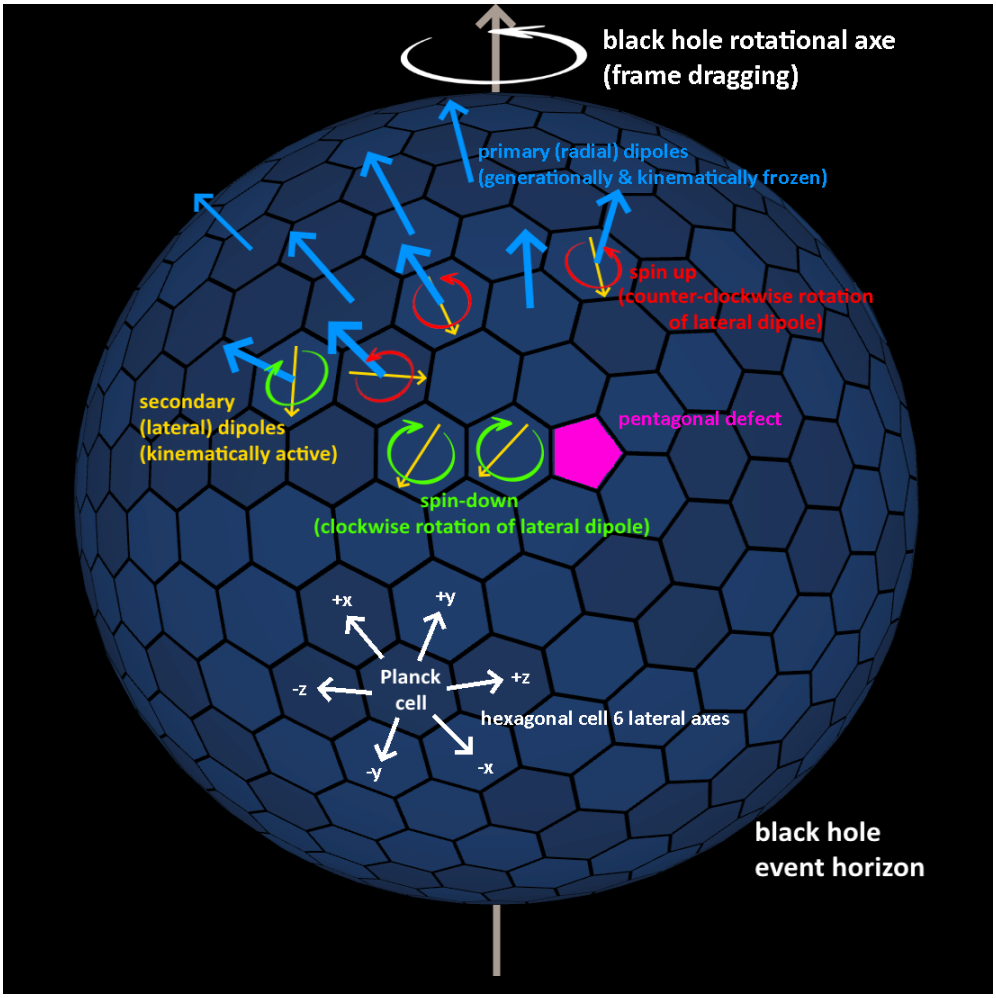

Fig. 6 Schematic representation of a Kerr black hole horizon surface composed of individual Planck cells. Hexagonal sphere created by @arscan.

5 Internal Universe Cosmology

In the horizon-layered cosmology, the classical Big Bang singularity is reinterpreted as the initial emergence of an effective internal spacetime encoded on (or reconstructed from) the near-horizon degrees of freedom of a black hole formed within a parent universe. Externally, the black hole may be described as beginning from a microscopic seed and growing through accretion. Internally, this growth is interpreted as an expansion whose earliest scales are set by Planck-level conditions in the horizon encoding. In this picture, the apparent origin of internal time corresponds to the progressive stratification and incorporation of infalling information into the horizon-layer

code: entropy and the available encoding capacity increase as new layers are added. This provides a qualitative route to extremely high effective initial densities in the reconstructed description without positing arbitrary bulk initial data.

In its earliest phase, the internal description is expected to be strongly coarse-grained. A Planck-scale (or near-Planck) horizon contains only $\mathcal{O}(1)$ cells around a great circle, corresponding to an extremely coarse angular resolution,

$$\Delta\phi_{\min} \sim \frac{\ell_{\rm p}}{r_{\rm s}} = \mathcal{O}(1)\,. \tag{140}$$

At such low encoding complexity, the reconstruction cannot support a detailed semi-classical field-theoretic description with many independently addressable angular modes. In this sense, the earliest internal epoch may be viewed as a "vacuum-like hologram" or pre-geometric regime, dominated by null-surface fluctuations and coarse-grained horizon noise rather than by a rich spectrum of stable, particle-like excitations.

As the parent horizon expands, the number of Planck-area cells grows as

$$\frac{A}{\ell_{\rm p}^2} \propto r_{\rm s}^2, \tag{141}$$

thereby improving angular resolution and permitting more elaborate patterns of horizon-side correlations to be represented. In this speculative view, the effective appearance of structured matter content and radiation in the internal description is tied not to arbitrary bulk initial conditions but to the increasing lateral encoding capacity of the horizon code as it grows. This suggests an analogy (at the level of qualitative staging) with the earliest epochs of standard cosmology, in which progressively lower-energy effective descriptions become applicable as the universe expands and cools.

In conventional cosmology, a brief period of exponential inflation is invoked to address the horizon and flatness problems and to generate nearly scale-invariant fluctuations [26, 27]. In the horizon-layered picture, one may instead speculate that early episodes of rapid horizon growth or global re-synchronization (e.g. due to strong accretion variability or merger events when the horizon was still small) could force substantial retessellations of the horizon-side code. From the internal perspective, such episodes could appear as transient "inflation-like" intervals in which correlation structure is rapidly reorganized and effective expansion temporarily departs from the late-time coasting behavior. Establishing whether such episodes can reproduce inflationary perturbation phenomenology requires a dedicated perturbation theory within the reconstruction and is not assumed here.

After any such early reorganizations, the internal universe is expected to enter a smoother adiabatic phase in which the parent horizon grows more steadily through accretion and minor mergers, yielding a stable effective Hubble flow in the reconstructed description. In this regime, cosmic expansion arises directly and continuously

from the growth of the parent black hole: each increment of accreted mass corresponds to the incorporation of a new null-ordered layer, triggering a global update of the horizon encoding and advancing internal time. The resulting expansion therefore does not require a separate inflaton field or a finely tuned vacuum-energy component at the level of this qualitative picture.

Within this framework, standard cosmological puzzles admit alternative interpretations. The horizon problem is softened because the reconstructed interior descends from a single, persistent boundary system whose degrees of freedom remain laterally causally connected on the stretched horizon, allowing global re-synchronization of the encoding even when the classical event horizon itself is a null surface. Flatness, in turn, is suggested to be associated with entropy-driven smoothing of the horizon-side code in the coarse-grained limit. The long-term expansion remains smooth and self-similar insofar as it is governed by the same horizon-based causal-scaling rule at successive updates.

The coexistence of global retessellation and local lateral propagation provides a unified narrative for both light propagation and cosmic expansion in the reconstructed interior. Each Planck-step incorporation adds a new layer of causal cells and reindexes the adjacency structure of the encoding lattice. In the internal description this appears as expansion: relational distances between encoded emitter and observer increase at every global update. A photon's wavelength is stretched not because it "loses" energy in flight, but because its propagating pattern is continuously re-embedded into an ever-larger horizon lattice; the observed redshift records the cumulative effect of these successive re-indexings.

Between global updates, the horizon lattice functions as a quasi-static causal medium. Within each such interval, photons propagate by sequential transfer of their encoded pattern across neighboring cells at the invariant null rate c. Internally, the combined effect of (i) local null propagation between updates and (ii) global retessellation at updates appears as continuous motion through a smoothly expanding spacetime.

Thus, a photon's apparent journey across the internal universe results from two intertwined processes: null propagation of its encoded pattern within each quasi-static causal frame, and global retessellation that expands the underlying relational geometry. In this interpretation, propagation and expansion are not independent phenomena but complementary aspects of a single discrete holographic process by which the horizon continuously re-encodes the causal structure of the reconstructed interior.

5.1 Universal Coasting Relation $H(t) \simeq 1/t$ and Revised Cosmic Time

In the horizon-layered reconstruction, cosmic time is not introduced as an independent background parameter but is identified operationally with the cumulative ordering of completed horizon-incorporation events. The emergent interior geometry is therefore parametrized by a single time variable tied to horizon growth, rather than to a prescribed bulk stress–energy evolution. This identification is part of the reconstruction

convention and should not be interpreted as a statement about fundamental time in the parent spacetime.

For a spherically symmetric parent black hole, the geometric Schwarzschild radius is

$$r_{\rm s} = 2M_{\rm bh}, \tag{142}$$

where $M_{\rm bh}$ denotes the black-hole mass expressed in *geometric units* (length units, with $G = c = 1$). The corresponding physical mass is

$$m_{\rm bh} = \frac{c^2}{G}\, M_{\rm bh}. \tag{143}$$

Internal time from completed incorporations.

Within the bookkeeping scheme adopted here, the internal cosmic time parameter is defined as the cumulative number of completed Planck-scale incorporation steps,

$$t \equiv g\, t_{\rm p}, \tag{144}$$

where g is the generational index and $t_{\rm p}$ the Planck time. Using the conservative identification that each completed update corresponds to an increment $\Delta M = \ell_{\rm p}$ in geometric mass, one obtains the kinematic identity

$$t = \frac{M_{\rm bh}}{c} = \frac{G m_{\rm bh}}{c^3} = \frac{r_{\rm s}}{2c}. \tag{145}$$

This relation is not a dynamical law; it is an internal consistency condition linking the chosen time parameter to cumulative horizon growth within the reconstruction.

Equation (145) implies

$$r_{\rm s}(t) = 2ct, \tag{146}$$

so that, in this bookkeeping description, the horizon radius grows linearly with the internal time parameter.

Hubble scale in the reconstructed interior.

In a spatially flat FLRW description, the Hubble radius is defined kinematically as

$$r_h(t) \equiv \frac{c}{H(t)}. \tag{147}$$

Within the horizon-layered reconstruction, the fractional-scaling convention adopted for the emergent interior geometry yields

$$H(t) \equiv \frac{\dot{a}}{a} = \frac{\dot{r}_{\rm s}}{r_{\rm s}}. \tag{148}$$

Using Eq. (146), one finds

$$\dot{r}_{\rm s} = 2c, \qquad \Rightarrow \qquad H(t) = \frac{1}{t}. \tag{149}$$

Thus the coasting relation

$$H(t) = \frac{1}{t} \tag{150}$$

emerges as a kinematic consequence of the chosen horizon-growth bookkeeping and fractional-scaling rule, rather than from a Friedmann equation with specified matter content.

The associated Hubble radius is therefore

$$r_h(t) = ct, \tag{151}$$

while the parent horizon radius satisfies

$$r_{\rm s}(t) = 2r_h(t). \tag{152}$$

This factor-of-two relation is a specific feature of the present reconstruction.

Effective density as a diagnostic quantity.

Once the FLRW envelope and $H(t)$ are fixed, one may introduce an effective energy density purely as a diagnostic reparameterization,

$$\rho(t) \equiv \frac{3}{8\pi G}\, H(t)^2 = \frac{3}{8\pi G t^2}, \tag{153}$$

corresponding formally to an effective equation-of-state parameter $w_{\rm eff} = -1/3$. No bulk stress–energy tensor is assumed or derived; this quantity merely encodes the reconstructed kinematics in standard cosmological notation.

Revised cosmic age.

Within this kinematic framework, the present cosmic age is inferred directly from the locally measured Hubble constant,

$$t_0 = \frac{1}{H_0}. \tag{154}$$

Using the SH0ES determination [28],

$$H_0 = 2.366 \times 10^{-18}\,{\rm s}^{-1}, \tag{155}$$

one finds

$$t_0 \simeq 4.23 \times 10^{17}\,{\rm s} \simeq 13.4\,{\rm Gyr}. \tag{156}$$

This value is close to, though not identical with, the age inferred in ΛCDM, reflecting the different operational definition of cosmic time employed here.

Horizon size and informational content.
Using Eq. (145), the present geometric mass associated with the parent horizon is

$$M_{\rm bh} = ct_0 \simeq 1.27 \times 10^{26}\,{\rm m}, \tag{157}$$

corresponding to a physical mass

$$m_{\rm bh} = \frac{c^2}{G} M_{\rm bh} \simeq 1.7 \times 10^{53}\,{\rm kg}, \tag{158}$$

and Schwarzschild radius

$$r_{\rm s} = 2M_{\rm bh} \simeq 2.5 \times 10^{26}\,{\rm m}. \tag{159}$$

The number of completed Planck-mass incorporations is

$$N_{\rm inc} = \frac{m_{\rm bh}}{m_{\rm p}} \sim 10^{61}, \tag{160}$$

while the number of Planck-area cells on the horizon is

$$N_{\rm cell} = \frac{A}{\ell_{\rm p}^2} = \frac{4\pi r_{\rm s}^2}{\ell_{\rm p}^2} \sim 10^{123}. \tag{161}$$

These quantities depend only on the horizon area and the fundamental constants $(G, \hbar, c)$ and therefore characterize the information capacity of the horizon independently of the interior reconstruction.

In summary, the relation $H(t) = 1/t$ appears in the horizon-layered framework as a direct consequence of the adopted horizon-growth bookkeeping and fractional scaling. It provides a simple coasting expansion law within the reconstructed FLRW envelope, without invoking dark energy, early-universe fine-tuning, or bulk dynamical assumptions.

5.2 FLRW Dynamics from Holographic Horizon Growth

In the horizon-layered cosmology, the expansion of the reconstructed interior follows from two complementary ingredients:

1. the *microscopic* growth of the parent horizon through discrete, Planck-scale incorporations, and
2. the *macroscopic* geometric identification between horizon radius and the internal cosmic time parameter.

Together, these ingredients yield an effective FLRW description of the interior spacetime without introducing an inflaton field, a dark-energy sector, or an assumed equation of state. All relations derived below are kinematic consequences of the reconstruction conventions rather than independent dynamical postulates.

1. Microscopic scaling from horizon growth. Each completed Planck-scale incorporation increases the Schwarzschild radius of the parent horizon by a fixed increment,

$$r_{\rm s}(t + t_{\rm p}) = r_{\rm s}(t) + 2\ell_{\rm p}, \tag{162}$$

reflecting the bookkeeping rule $\Delta M = \ell_{\rm p}$ in geometric units. Isotropy of the reconstructed interior requires that all comoving radial labels be rescaled by the same fractional factor after each completed update,

$$\lambda(t) = 1 + \frac{2\ell_{\rm p}}{r_{\rm s}(t)}. \tag{163}$$

In the continuum limit, this induces the fractional growth law

$$\frac{\dot{r}_{\rm s}}{r_{\rm s}} = \frac{2\ell_{\rm p}}{r_{\rm s}(t)}\,\frac{1}{t_{\rm p}} = \frac{2c}{r_{\rm s}(t)}, \tag{164}$$

where $\ell_{\rm p}/t_{\rm p} = c$ has been used. Microscopic horizon growth thus defines an effective expansion rate

$$H(t) \equiv \frac{\dot{a}}{a} = \frac{2c}{r_{\rm s}(t)}. \tag{165}$$

2. Macroscopic geometric identification. Within the reconstruction, the internal cosmic time parameter is identified operationally with cumulative horizon growth,

$$t = \frac{r_{\rm s}}{2c}. \tag{166}$$

This relation is definitional rather than dynamical. It implies

$$r_{\rm s}(t) = 2ct \qquad \Rightarrow \qquad \frac{2c}{r_{\rm s}(t)} = \frac{1}{t}. \tag{167}$$

Substituting into Eq. (165) yields

$$H(t) = \frac{1}{t}, \tag{168}$$

which holds throughout the reconstructed interior as a kinematic consequence of horizon growth and the chosen time normalization.

3. Scale factor behavior. Since all comoving distances are rescaled proportionally to the horizon radius, the effective FLRW scale factor satisfies

$$\frac{\dot{a}}{a} = H(t) = \frac{1}{t}, \tag{169}$$

with solution

$$a(t) = a_0\, t, \tag{170}$$

where a_0 is a normalization constant fixed by convention. The reconstructed interior therefore exhibits linear (coasting) expansion in cosmic time.

4. Effective density scaling. The total mass associated with the reconstructed interior grows linearly with the number of completed incorporations, so that $m(t) \propto t$. The associated effective energy density, introduced purely as a diagnostic quantity,

$$\rho(t) = \frac{m(t)}{\frac{4\pi}{3} r_{\mathrm{s}}(t)^3}, \tag{171}$$

then scales as

$$\rho(t) \propto \frac{1}{t^2}. \tag{172}$$

Using $a(t) \propto t$, this may be written equivalently as

$$\rho(t) \propto a(t)^{-2}. \tag{173}$$

No physical bulk stress–energy tensor is assumed; this density simply re-expresses the reconstructed kinematics in standard cosmological notation.

5. Spatial curvature. Interpreting the reconstructed relations through the standard FLRW diagnostic identity,

$$H^2 = \frac{8\pi G}{3}\rho - \frac{k}{a^2}, \tag{174}$$

and substituting $H \propto t^{-1}$ and $\rho \propto t^{-2}$ yields

$$k = 0. \tag{175}$$

The reconstructed interior is therefore spatially flat,

$$k = 0, \tag{176}$$

as a direct consequence of the area–volume scaling inherent in the holographic construction.

6. Consolidated FLRW correspondence. The horizon-layered reconstruction yields the effective relations

$$H(t) = \frac{1}{t}, \qquad a(t) \propto t, \qquad \rho(t) \propto a^{-2}, \qquad k = 0. \tag{177}$$

These relations are not imposed as field equations but arise simultaneously from discrete horizon growth and the geometric identification $r_{\mathrm{s}} = 2ct$.

Summary. In the horizon-layered cosmology, linear expansion, spatial flatness, and the characteristic a^{-2} density scaling emerge as kinematic consequences of null-ordered horizon growth and scale-free reconstruction conventions. The resulting FLRW behavior reflects properties of the holographic boundary and its growth history, rather than the dynamics of a bulk matter field or vacuum-energy component.

5.3 Resolution of the Vacuum Catastrophe through Holographic Encoding

A standard zero-point estimate in quantum field theory assigns to the vacuum an energy density

$$\rho_{\rm vac}^{\rm qft} \sim \int^{k_{\rm max}} \frac{d^3k}{(2\pi)^3}\,\frac{1}{2}\hbar\omega_k \sim \int^{1/\ell_p} k^3\,dk \sim \frac{\hbar c}{\ell_p^4}. \tag{178}$$

This estimate depends only on the ultraviolet cutoff ℓ_p and is independent of the size or curvature scale of the universe. It exceeds the observed cosmological vacuum density by approximately 10^{120}–10^{123}, the well-known "vacuum catastrophe." In conventional QFT this discrepancy arises because each Planck-scale volume element in the bulk is treated as an independent contributor to gravitational energy density.

In the horizon-layered cosmology, this discrepancy is reinterpreted as a form of *causal overcounting*. Quantum vacuum fluctuations are not denied; rather, the claim is that their net gravitational effect is constrained by holographic principles. Only degrees of freedom that are causally registered at the horizon, and hence participate in the null-ordered updating of the holographic boundary, are taken to contribute to large-scale curvature. Volumetric mode counting therefore overestimates the gravitationally relevant vacuum energy. In this framework, the physically operative degrees of freedom scale with horizon area rather than with bulk volume.

The contrast between $\rho_{\rm vac}^{\rm qft}$ and the observed value thus reflects the difference between volumetric ultraviolet counting and holographic causal counting, with an effective density of order one degree of freedom per Planck-area cell.

Using the present horizon parameters obtained earlier,

$$m_{\rm bh} \simeq 1.7 \times 10^{53}\ {\rm kg}, \qquad r_{\rm s} \simeq 2.5 \times 10^{26}\ {\rm m}, \tag{179}$$

the cumulative number of Planck-mass incorporations and the number of Planck-area cells are

$$N_{\rm inc} = \frac{m_{\rm bh}}{m_{\rm p}} \sim 10^{61}, \qquad N_{\rm cell} = \frac{4\pi r_{\rm s}^2}{\ell_{\rm p}^2} \sim 10^{123}. \tag{180}$$

The observed vacuum density is set by the large-scale curvature scale,

$$\rho_{\rm vac}^{\rm obs} \sim \frac{3H^2}{8\pi G} \sim \frac{c^2}{G r_{\rm s}^2}, \tag{181}$$

where the second relation uses the coasting identification $H \sim c/r_{\rm s}$. The ratio of the naive QFT estimate to the observed value is therefore

$$\frac{\rho_{\rm vac}^{\rm qft}}{\rho_{\rm vac}^{\rm obs}} \sim \frac{\hbar c/\ell_p^4}{c^2/(G r_s^2)} \sim \frac{r_s^2}{\ell_p^2} = N_{\rm cell}. \tag{182}$$

Thus the enormous discrepancy between naive QFT estimates and observations numerically coincides with the number of Planck-area cells on the

cosmological horizon. In this interpretation, quantum field theory effectively counts all ultraviolet modes as independent sources of curvature, whereas the holographic framework limits gravitational relevance to causally accessible boundary degrees of freedom.

If the gravitationally relevant vacuum contribution is associated with the infrared curvature scale of the horizon rather than with bulk ultraviolet fluctuations, one obtains parametrically

$$\rho_{\rm vac} \sim \kappa \, \frac{c^4}{8\pi G r_{\rm s}^2}, \tag{183}$$

where $\kappa = \mathcal{O}(1)$ encodes details of horizon definition and coarse graining. The r_s^{-2} scaling appears in a variety of independent contexts, including de Sitter thermodynamics, holographic dark-energy models, and emergent-gravity approaches [29–32].

Numerically, for $r_{\rm s} \simeq 2.5 \times 10^{26}\,{\rm m}$,

$$\rho_{\rm vac}(\kappa{=}1) \approx 8 \times 10^{-28}\ {\rm kg\,m^{-3}}, \tag{184}$$

which lies within an order of magnitude of the observed cosmological vacuum density. Modest $\mathcal{O}(1)$ variations in κ account for the precise numerical coefficient.

Interpretation. In this speculative framework, vacuum energy is interpreted not as the energy of empty space per se, but as an effective curvature cost associated with maintaining a finite information density at the causal boundary. As the horizon grows and its area increases, the curvature contribution per degree of freedom decreases as r_s^{-2}. The observed late-time acceleration is therefore re-expressed as a boundary-scale effect tied to horizon growth rather than as evidence for a large bulk vacuum instability.

In summary, the vacuum catastrophe is reformulated as a mismatch between bulk ultraviolet mode counting and holographic causal accounting. Within the horizon-layered cosmology, the cosmological constant functions as an effective bookkeeping parameter for horizon information density, controlled by the finite causal bandwidth of the null boundary rather than by unconstrained ultraviolet bulk physics.

5.4 Redshift Relations, Temporal Scaling, and Implications for Early-Universe Timing

In the horizon-layered cosmology, cosmic time is defined operationally through the null-ordered growth of a holographic horizon rather than through the dynamical evolution of a metric scale factor. With the identification $r_{\rm s}(t) = 2ct$, the redshift of freely propagating massless signals can be expressed kinematically as a ratio of horizon-encoded timescales,

$$1 + z = \frac{\nu_{\rm em}}{\nu_{\rm obs}} = \frac{g_{\rm obs}}{g_{\rm em}} = \frac{r_{\rm s}(t_0)}{r_{\rm s}(t_z)} = \frac{t_0}{t_z}, \tag{185}$$

where t_0 denotes the present internal time and t_z the internal time associated with emission at redshift z. This yields the causal time–redshift relation

$$\boxed{t_z = \frac{t_0}{1+z}.} \tag{186}$$

This relation follows directly from horizon growth and pointer drift and differs from the standard FLRW mapping between redshift and cosmic time. Importantly, all observable redshifts are preserved; only their temporal interpretation within the reconstruction is modified.

Differentiating with respect to time gives the corresponding redshift dependence of the Hubble parameter,

$$\boxed{H(z) = \frac{1+z}{t_0},} \tag{187}$$

with $t_0 = 1/H_0$ by construction. In this framework, the present-day Hubble constant fixes the overall normalization of internal time.

Maximum causal redshift. The earliest meaningful internal time is the Planck time t_{p}, which sets a formal upper bound on causal compression,

$$1 + z_{\max} = \frac{t_0}{t_{\mathrm{p}}}, \qquad z_{\max} \sim 10^{61}. \tag{188}$$

This quantity should not be interpreted as a physical emission redshift but as a limit of the null-ordered encoding underlying the reconstruction.

Implications for early-universe timing. In standard ΛCDM cosmology, the conversion between redshift and cosmic time is fixed by the Friedmann equations and early-universe matter content. In the horizon-layered framework, the mapping $t(z) = t_0/(1+z)$ instead reflects the growth history of the horizon. As a result, events conventionally assigned to very early cosmic times are placed later in internal time, while leaving their observed redshifts unchanged.

For example, using $z_{\mathrm{CMB}} = 1089.92$ and $t_0 = 4.23 \times 10^{17}\,\mathrm{s}$,

$$t_{\mathrm{CMB}} = \frac{t_0}{1+z_{\mathrm{CMB}}} \simeq 3.9 \times 10^{14}\,\mathrm{s} \approx 12\ \mathrm{Myr}. \tag{189}$$

In this reconstruction, the surface of last scattering is therefore associated with an internal time of order tens of Myr rather than hundreds of kyr. This does not alter the observed CMB spectrum or angular correlations, but it changes the interpretation of how much internal time is available before recombination.

Thermal scaling and causal saturation. The standard temperature scaling $T = T_0(1+z)$ diverges formally as $z \to \infty$. Within a holographic setting, it is natural to expect this growth to be limited by causal and informational bounds. As a

phenomenological interpolation, one may introduce the saturation form

$$T(z) = \frac{T_{\mathrm{P}}\, T_0(1+z)}{T_{\mathrm{P}} + T_0(1+z)}, \tag{190}$$

which reproduces the standard relation at low redshift and asymptotes to the Planck temperature T_{P} at early times. This expression should be regarded as an effective parametrization rather than a derived thermodynamic law.

At recombination, the correction is negligible, yielding

$$T_{\mathrm{CMB}} \approx 3 \times 10^3 \text{ K}, \tag{191}$$

consistent with standard recombination physics.

Early structure formation. Recent observations of massive galaxies at redshifts $z \gtrsim 10$–14 suggest that substantial structure formation occurred at relatively early epochs. Under the horizon-layered time–redshift relation,

$$t(z = 14.44) = \frac{13.4 \text{ Gyr}}{15.44} \approx 0.87 \text{ Gyr}, \tag{192}$$

providing substantially more internal time for early star formation and chemical evolution than in the standard ΛCDM time assignment. This alleviates, though does not by itself resolve, the tension between early structure formation and conventional growth timescales.

Epoch	**Standard ΛCDM time**	**Horizon-layered time**
Present ($z = 0$)	13.8 Gyr	13.4 Gyr
First galaxies ($z = 14.44$)	~ 0.28 Gyr	~ 0.87 Gyr
CMB ($z = 1089.92$)	~ 0.38 Myr	~ 12 Myr

Interpretation. Within this speculative framework, redshift is interpreted as a measure of temporal encoding across successive null-synchronized horizon layers rather than as a direct proxy for metric expansion alone. The modified time–redshift relation,

$$t(z) \propto (1+z)^{-1}, \tag{193}$$

offers an alternative causal interpretation of early-universe timing while leaving all directly observed redshift-dependent quantities unchanged.

In summary, the horizon-layered reconstruction provides a self-consistent reinterpretation of cosmic timing that may soften apparent tensions associated with early structure formation. These results are intended as kinematic implications of the reconstruction rather than as a replacement for the successful phenomenology of standard cosmology.

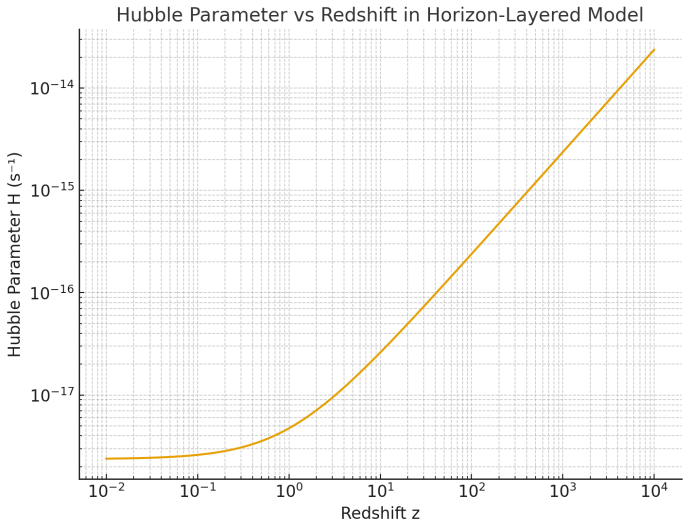

Fig. 7 Hubble parameter as a function of redshift in the horizon-layered cosmology. The plotted curve shows the linear relation $H(z) = \frac{1+z}{4.2265427\times10^{17}}$ s^{-1}, predicted by the causal incorporation model, with the redshift z expressed on a logarithmic scale. In this framework, the Hubble parameter is not governed by energy-density dilution as in standard ΛCDM cosmology, but arises directly from the discrete, constant incorporation of information quanta across the holographic horizon. The expansion of space corresponds to the cumulative growth of internal time, $H = 1/t$, where t measures the total number of successful incorporations since the initial horizon formation. Thus, the apparent decrease of H with cosmic time does not signify a slowing of dynamics or matter dilution, but simply reflects the increasing temporal depth of the internal universe as more information is encoded. The incorporation rate itself remains fixed at one quantum per Planck tick, defining the universal causal rhythm underlying cosmic expansion.

5.5 Topological Defects, Kerr Coupling, and Large-Scale Anisotropies

In the horizon-layered cosmology, the holographic boundary is a finite, closed, two-dimensional null surface discretized into Planck-area cells. For any approximately uniform tiling of the sphere by locally hexagonal cells, global topology imposes unavoidable defects. By Euler's theorem, a closed spherical tessellation must contain a net positive curvature deficit, realized most economically by twelve pentagonal cells embedded in an otherwise hexagonal lattice. These defects are not imperfections of the construction but topological invariants of the closed surface.

Each horizon cell participates in null-synchronized lateral information exchange with its neighbors. Hexagonal cells possess six nearest neighbors, while pentagonal cells possess only five, producing a local deficit in lateral connectivity. As a result, the adjacency graph of the horizon carries localized curvature concentrations at the defect sites. Because horizon excitations propagate tangentially through this graph, pentagonal cells introduce small but irreducible anisotropies in phase-coherent null propagation. These anisotropies are globally constrained and cannot be removed by local retessellation.

Although the number of topological defects is fixed and small, the horizon code is updated globally at every Planck-scale incorporation step during the early growth of the parent horizon. During these early epochs, when the horizon radius is smallest, defect-induced distortions constitute the largest fractional departure from perfect isotropy. Consequently, the shallowest generational layers preferentially encode long-wavelength modes of the reconstructed interior. Under holographic projection, these modes contribute dominantly to the lowest angular multipoles of the emergent cosmology.

This mechanism naturally associates horizon topology with large-angle anisotropies in the cosmic microwave background. Suppression of power at the lowest multipoles, mild alignment of low-ℓ modes, parity asymmetries, and hemispherical modulations may arise as coherent imprints of the fixed defect configuration rather than as statistical fluctuations of an exactly Gaussian field. Because the defect structure is global and topologically protected, its imprint is concentrated at large angular scales while leaving small-scale statistics approximately isotropic.

The hierarchy of scales is extreme. The number of Planck-area cells is currently

$$N_{\rm cell} = \frac{A}{\ell_{\rm p}^2} \sim 10^{123}, \tag{194}$$

while the number of topological defects remains $\mathcal{O}(10)$. The raw fractional defect contribution at the horizon scale is therefore minuscule. However, holographic projection and subsequent expansion map this fixed defect pattern preferentially onto the largest observable angular modes, where it need not be small relative to cosmic variance. This naturally yields order-unity effects at $\ell \lesssim \mathcal{O}(10)$ and negligible impact at high ℓ.

At the epoch corresponding to last scattering in this framework,

$$t_{\rm CMB} \simeq 12 \text{ Myr}, \qquad t_0 \simeq 13.4 \text{ Gyr}, \tag{195}$$

the ratio of horizon radii satisfies

$$\frac{r_{\rm s}(t_0)}{r_{\rm s}(t_{\rm CMB})} = \frac{t_0}{t_{\rm CMB}} = 1 + z_{\rm CMB} \simeq 1090. \tag{196}$$

The defect pattern is therefore comoving: its angular structure is preserved under expansion, while its physical scale is redshifted. This ensures that defect-induced anisotropies remain confined to the lowest multipoles at late times.

If the parent black hole carries angular momentum, the horizon acquires an additional global structure. In the Kerr geometry, null generators of the horizon rotate with angular velocity

$$\Omega_H = \frac{c^3}{2Gm_{\rm bh}} \frac{\chi}{1+\sqrt{1-\chi^2}}, \qquad \chi = \frac{cJ}{Gm_{\rm bh}^2}. \tag{197}$$

This rotation introduces a systematic azimuthal phase gradient across the horizon lattice. Topological defects embedded in such a rotating background inherit a preferred

orientation relative to the spin axis, rendering the global defect configuration weakly chiral.

Under holographic reconstruction, this combined topological and rotational structure can introduce directional asymmetries and parity-sensitive effects in the largest-scale cosmological observables. Low-ℓ mode alignments, hemispherical power asymmetry, and parity-odd correlations may therefore reflect rotational memory of the parent horizon rather than statistical anomalies or late-time foregrounds. The preferred axis defined by such effects is expected to remain stable across datasets, as it is anchored to horizon topology and angular momentum rather than to stochastic initial conditions.

Because the horizon-layered cosmology does not invoke a slow-roll inflaton or a separate early-time scalar sector, it does not generically predict a large stochastic background of primordial gravitational waves. Tensor modes, if present, arise from horizon retessellation and defect dynamics and are therefore expected to be small, anisotropic, and correlated with large-scale temperature and polarization features. The effective tensor-to-scalar ratio is expected to be well below current observational bounds, with any detectable signal confined to very low multipoles.

In summary, unavoidable topological defects of a closed holographic horizon, possibly coupled to rotational memory of a Kerr progenitor, provide a natural source of coherent large-scale anisotropies. Within the horizon-layered framework, several observed low-ℓ features of the cosmic microwave background can be interpreted as fossil imprints of horizon topology rather than as statistically unlikely fluctuations. These effects are confined to the largest angular scales and do not disrupt the near-isotropy and Gaussianity of small-scale cosmological observables.

5.6 Merging Black Holes and Internal Causal Reconfiguration

In the horizon-layered cosmology, a black-hole merger corresponds to a reorganization of the parent horizon's null-ordered encoding. Each black hole carries its own horizon structure and causal ordering associated with its growth history. When two horizons merge, these orderings do not combine additively. Instead, they re-synchronize into a single enlarged horizon with a unified null-ordering structure. Externally, this process is described by horizon coalescence and gravitational wave emission; internally, it corresponds to a global retessellation of the null-surface code.

The external description obeys the classical area theorem,

$$A_{\text{after}} \;>\; A_1 + A_2, \tag{198}$$

so the entropy associated with the merged horizon necessarily increases. The enlarged horizon therefore possesses a greater information capacity, and the internal causal domain reconstructed from it expands accordingly.

Global renormalization of horizon weights. A key operational requirement of the reconstruction is that the mass–per–cell weights associated with Planck-scale horizon elements must be consistent with the *final* total horizon area. If the weights inherited from the progenitor horizons were retained unchanged, the merged horizon would

encode an inconsistent mass and entropy. To preserve saturation of the holographic bound and a smooth null ordering, the entire horizon undergoes a global re-indexing in which all cells are assigned weights appropriate to the final mass M_{after}. This renormalization is not a dynamical process acting within the interior, but a bookkeeping adjustment required for a consistent boundary encoding.

Within this framework, no independent "sub-horizons" or autonomous internal domains associated with the progenitor black holes survive. The merged horizon defines a single, unified causal structure from which a single interior reconstruction is obtained.

Early-stage mergers. When the parent horizon is small, mergers can produce large fractional increases in area. The associated retessellation of the horizon is then strongly non-adiabatic in the sense that a large number of Planck-scale incorporations must be re-synchronized over a short external timescale. In the internal reconstruction, such episodes correspond to rapid changes in the null-ordering structure. These early reconfigurations provide a natural mechanism for generating long-wavelength perturbations and departures from perfect homogeneity, without invoking a separate inflaton field or potential-driven dynamics.

Late-stage mergers. In the mature regime relevant to the present universe, the parent horizon is enormously massive. For a parent mass m_{parent}, the fractional change in horizon area due to the merger with a black hole of mass Δm scales as

$$\frac{\Delta A}{A} \sim 2\,\frac{\Delta m}{m_{\text{parent}}}. \tag{199}$$

Even mergers involving astrophysically large black holes then produce extremely small fractional changes. The resulting retessellation is effectively adiabatic: the null ordering adjusts smoothly, and no sharp features are introduced into the reconstructed interior.

Internal continuity. Because the renormalization of horizon weights is global, the reconstructed interior geometry adjusts coherently at all scales. Relative changes in effective expansion rate or curvature are suppressed by the small ratio $\Delta m/m_{\text{parent}}$. In the late-time regime, such adjustments are negligible, and the interior remains well described by a smooth FLRW-like geometry. Astrophysical mergers that are dramatic in the external description therefore correspond, internally, to imperceptibly slow changes in global parameters.

Cosmological chronology. The reconstruction naturally separates the internal history into two broad phases:

1. *Early non-adiabatic phase:* frequent mergers and rapid horizon growth produce significant retessellations and imprint large-scale perturbations.
2. *Late adiabatic phase:* the parent horizon becomes so large that individual merger events contribute negligibly to its total area, yielding a smooth and stable internal evolution.

The observed isotropy and gentle late-time expansion of the universe are consistent with reconstruction from a horizon in this mature regime.

Residual signatures. Perturbations seeded during early non-adiabatic reconfigurations may survive as large-scale anomalies or low-multipole features in cosmological observables. Later mergers, by contrast, leave no detectable internal signatures. In this sense, the present universe retains only fossil evidence of its earliest horizon-growth history.

In summary, black-hole mergers correspond, within the horizon-layered framework, to global reorganizations of the holographic boundary whose internal significance depends on the evolutionary stage of the parent horizon. Early mergers can imprint large-scale structure, while late mergers are adiabatic and effectively invisible in the reconstructed interior. A single, self-consistent causal domain always emerges, ensuring continuity and smoothness of the internal cosmology.

6 Multiverse and Holographic Hierarchies

During gravitational collapse, the forming event horizon becomes a causal boundary separating the exterior universe from an interior domain generated by null-surface dynamics. In the present framework, the internal cosmology associated with a black hole is not treated as a pre-existing spacetime, but as a holographic reconstruction encoded on the evolving horizon. As infalling quanta reach the stretched horizon, they are incorporated through Planck-scale updates, and the resulting sequence of null layers defines the initial conditions and subsequent evolution of an emergent interior description. The classical singularity is replaced, at the operational level, by a causal and informational origin: a boundary from which spacetime structure is reconstructed.

A parent universe may contain a large population of black holes, primordial, stellar-mass, or supermassive, each potentially associated with its own internal reconstruction. Within this interpretation, each black hole acts as a node in a generative hierarchy, with the effective properties of any reconstructed universe reflecting the accretion history and null-layer structure of its parent horizon. The resulting architecture may be viewed as a recursively nested multiverse, in which each level inherits its initial conditions from the causal encoding of the preceding one.

This picture resonates with earlier ideas of baby-universe formation [33, 34], but reinterprets black holes as holographic generators whose horizons encode the causal blueprint of their descendants. According to the classical no-hair theorem, a black hole is externally characterized only by mass, charge, and angular momentum [20]; in the holographic interpretation, however, its full set of quantum correlations may encode additional internal causal structure that is invisible to asymptotic observers.

Horizon cells as the primitive substrate of spacetime. At the Planck scale, the horizon is modeled as a discrete causal lattice. Each Planck-area cell represents a primitive correlation unit whose links to neighboring cells may be complete, partial, or absent. Complete links yield smooth causal propagation and define continuum geometry, while incomplete links reduce local causal capacity and manifest externally as curvature and gravitational mass. Spacetime is thus treated as an emergent network of correlations rather than a fundamental manifold. The horizon evolves subject to a maximal causal throughput $P_{\max} = c^5/G$, continually reorganizing its correlations to maintain global consistency.

Within this framework, the horizon functions as an effective terminal null layer for the exterior description, rather than as a surface concealing a physical singularity. No internal observer can access or probe the parent horizon directly, since the reconstructed spacetime is generated from its causal ordering. The Bekenstein–Hawking entropy bounds the total information capacity available for any such reconstruction [10].

A recursively generated multiverse. Although each black hole may be associated with a new internal reconstruction, the number of distinct causal domains derivable from a given horizon is bounded by its entropy budget. Recursive generation is therefore constrained at each level by finite information capacity, yielding causally disjoint descendant domains. Universes that fail to maintain stable causal encoding or cannot form black holes produce no further descendants, while those that do may give rise to

additional levels. This resembles cosmological natural selection [33], here expressed in holographic terms as a selection for stable causal-encoding structures.

In this view, our observable universe is interpreted as an emergent interior reconstruction associated with a boundary located just above a parent horizon. The internal spacetime does not coexist with that boundary within the same geometric domain; rather, the boundary belongs to a higher-order spacetime that is causally inaccessible from within. Operationally, the event horizon functions not as a surface embedded in our universe, but as the outermost null layer that defines its causal ordering.

Ultimate horizons and the hierarchy of time. If the holographic hierarchy possesses an uppermost member, a causal boundary that admits no external accretion, its evolution would differ qualitatively from that of its descendants. Without inflow, such an *ultimate horizon* could not grow through external incorporation, and its dynamics would be driven solely by intrinsic lateral reconfigurations of causal adjacency in a closed null lattice. Within the speculative framework considered here, rare self-reindexing events may occur to preserve global coherence, providing a minimal notion of temporal ordering even in the absence of accretion.

By contrast, descendant universes obtain their temporal progression from accretion-driven incorporations. Each completed incorporation advances the internal causal order and yields a discrete increment of internal time. If accretion ceases, internal time, as defined operationally, likewise ceases to advance. The ultimate horizon, if it exists, would therefore define a higher-order temporal substrate from which descendant time orderings are inherited.

From the internal viewpoint, accretion-driven incorporations occur at a normal cosmic pace; relative to the sparse intrinsic updates of an ultimate horizon, however, each internal tick would correspond to an extended interval. Time thus appears not as an absolute flow, but as a relative measure of causal update density across layers of the holographic hierarchy.

Correlation as the foundation of physical reality. In this model, physical phenomena, matter, fields, and geometry, arise from evolving patterns of correlation among horizon cells. Spacetime is not the arena in which these patterns exist, but the effective projection of their causal ordering. The multiverse is therefore represented as a hierarchy of projected correlation structures, each constrained by the informational capacity of its predecessor. Dimension, mass, and curvature are emergent descriptors rather than fundamental entities.

The arrow of time as inherited causal order. Each newly incorporated horizon layer records an irreversible causal update, increasing total entropy and defining a directed sequence of events. Because each descendant reconstruction inherits its causal ordering from the layered structure of its parent, temporal asymmetry propagates recursively through the hierarchy. The arrow of time is thus not imposed as an initial condition, but emerges as an inherited property of the holographic generation process, the persistent memory of causal ordering encoded in horizons.

6.1 Apparent Quantum Randomness and Deterministic Parent Horizons

In conventional quantum mechanics, randomness is treated as intrinsic: measurement outcomes are assumed to occur without underlying determinism. In the horizon-layered cosmology, this interpretation is replaced by a causal–informational hierarchy in which quantum indeterminacy emerges from limited access to a deeper causal process.

Each universe in the holographic hierarchy is the internal projection of a parent horizon. From the parent frame, each Planck-scale incorporation event constitutes a definite causal update: a discrete, ordered addition of information–energy to the horizon encoding. From within the emergent internal spacetime, however, these same updates appear as probabilistic quantum events. The apparent stochasticity of measurement outcomes arises because observers inside the reconstructed universe have access only to a coarse-grained projection of the underlying null-ordered sequence.

In this framework, quantum randomness is interpreted as *epistemic rather than ontic*. It reflects informational coarse-graining imposed by the holographic boundary, not necessarily fundamental indeterminism. The deterministic or causally complete evolution of the parent horizon produces, under projection, the statistical behavior described internally by the Born rule,

$$P_{\text{internal}}(i) \;\sim\; \left|\langle i \,|\, \psi_{\text{encoded}}\rangle\right|^2, \tag{200}$$

where $|\psi_{\text{encoded}}\rangle$ denotes the effective boundary state associated with a given sequence of horizon incorporations. This relation is interpretive rather than derivational: the horizon-layered framework does not claim to derive the Born rule, but to offer a causal perspective from which its probabilistic structure may be understood as an emergent description.

Rotation of the parent horizon, characterized by the Kerr parameter $a = J/(Mc)$, introduces an additional geometric structure into the encoding. Frame dragging induces an azimuthal phase gradient across the horizon degrees of freedom, biasing the incorporation of co-rotating and counter-rotating modes. Over many incorporations, such geometric bias may manifest internally as small asymmetries in outcome statistics, including parity violation or matter–antimatter imbalance. Individual quantum events remain unpredictable to internal observers, but their ensemble properties may retain a weak imprint of the parent horizon geometry.

Causal closure. If the holographic hierarchy is finite, its highest level corresponds to a causally closed parent horizon: a null-ordered encoding that admits no further external boundary. At that level, the encoding dynamics are internally complete within the model. Quantum randomness in descendant universes would then arise from their embedded position within the hierarchy, rather than from fundamental indeterminism. This interpretation does not assert absolute determinism of nature, but causal completeness relative to the encoding structure assumed in the framework.

Finiteness of the hierarchy. Within the horizon-layered cosmology, a finite hierarchy is sufficient to ensure causal closure and consistency with holographic entropy bounds. An infinite regress of parent horizons is neither required nor favored by the construction, as each horizon possesses finite information capacity. However, the framework does not claim to exclude infinite structures on purely logical grounds; rather, it adopts finiteness as a minimal assumption compatible with entropy bounds and causal completeness.

Multiplicity of ultimate horizons. While each causal lineage may terminate in a finite parent horizon, multiple such lineages may coexist independently. These ultimate horizons would be causally disjoint, with no exchange of information between them. Such multiplicity does not violate holographic principles, provided each domain respects its own entropy bound. The framework remains agnostic as to whether the number of such ultimate horizons is finite or infinite.

In this speculative interpretation, the deepest layer of physical description is not characterized by observable randomness but by a causally ordered encoding structure. Quantum randomness, as experienced within our universe, arises as a coarse-grained manifestation of horizon-based causal dynamics that remain inaccessible to internal observers.

6.2 Cosmic Freeze-Out, Evaporation, and Horizon-Defined Time

A central implication of the horizon-layered framework is that internal cosmic time is not tied exclusively to horizon growth, but more generally to the ordered sequence of *global horizon retessellation events* by which the null surface updates its geometric and informational state. Each such retessellation corresponds to a discrete change of one geometric Planck mass unit in the horizon bookkeeping and advances internal time by one Planck interval,

$$t_{\mathrm{int}} = N_{\mathrm{ret}}\, t_{\mathrm{p}}, \tag{201}$$

where N_{ret} counts the total number of completed retessellations, irrespective of whether they arise from mass accretion or mass loss.

Growth phase: accretion-driven time. During epochs of active accretion, each completed incorporation of one geometric Planck mass unit increases the horizon area, triggers a global retessellation of the null surface, and advances internal time by one Planck tick. In this regime, horizon growth, retessellation, internal time, and effective cosmic expansion are tightly coupled. The reconstructed interior exhibits an expanding FLRW envelope whose scale factor tracks the cumulative horizon growth.

Evaporation phase: Hawking-driven time. When accretion becomes negligible and Hawking radiation dominates, the direction of mass flow reverses. Outgoing Hawking quanta originate entirely in the exterior near-horizon region, but their emission is accompanied by a corresponding decrease in the geometric mass encoded on the horizon. Each loss of one geometric Planck mass unit reduces the horizon area by $\Delta A \sim -16\pi r_s \ell_{\mathrm{p}}$ and likewise triggers a global retessellation of the horizon lattice.

Crucially, these evaporation-induced retessellations *also advance internal time by one Planck interval*. Internal time therefore continues to progress during evaporation,

$$\Delta m = \pm m_{\mathrm{p}} \quad \Longrightarrow \quad \Delta t_{\mathrm{int}} = t_{\mathrm{p}}, \tag{202}$$

independent of the sign of the mass change. Accretion and evaporation are thus treated symmetrically as horizon updates with opposite geometric effect but identical temporal weight.

Freeze-out as external description, not internal cessation. From the external perspective, both accretion and evaporation near the horizon are subject to extreme gravitational redshift. If accretion halts for an extended external duration, horizon retessellations become exceedingly sparse when measured in asymptotic time. This produces an apparent "freeze-out" of internal evolution as viewed from infinity.

Internally, however, no such freeze-out is observable. All physical processes, clocks, field dynamics, and correlations inside the reconstructed bulk are defined relative to the same sequence of horizon retessellations. When retessellations occur infrequently, all internal rates slow uniformly; when they occur more frequently, all rates accelerate uniformly. Because no internal clock exists that is not synchronized to the horizon updates, internal observers cannot detect whether retessellations are dense, sparse, or temporarily absent in external time. Operationally, time always proceeds normally whenever it proceeds at all.

Late-time behavior and disappearance of the interior. As Hawking evaporation continues, the horizon shrinks through successive negative mass retessellations. The reconstructed interior correspondingly contracts: spatial volumes decrease, cosmic structures unwind, and the effective FLRW domain shrinks toward zero size. Internal time continues to advance during this contraction phase, driven by the same Planck-scale bookkeeping as during growth.

When the horizon area reaches zero, no further retessellations are possible. At that point, the horizon ceases to exist as a causal encoding surface, and the reconstructed interior spacetime terminates. There is no residual interior region, frozen remnant universe, or detached causal domain. The disappearance of the horizon and the disappearance of the interior are the same physical event described from different reconstructions.

Unified picture. In this speculative framework, cosmic time is neither tied to expansion nor to accretion alone. It is the ordered count of horizon retessellations induced by discrete changes in geometric mass. Accretion drives expanding interiors; evaporation drives contracting interiors; both advance time identically. What appears externally as long quiescent periods or asymptotic evaporation corresponds internally to uninterrupted temporal flow, because time is defined relationally by horizon updates rather than by external duration.

Thus, the birth, evolution, contraction, and ultimate disappearance of an internal universe are unified as phases of a single horizon-governed causal process.

7 Conclusion

This paper has developed a new paradigm in which gravitational collapse is reinterpreted as a cosmogenic process. Taking the external observer's frame as physically authoritative, the event horizon ceases to be a passive geometric boundary and becomes an active, information-bearing null surface that encodes infalling matter into redshift-frozen, causally ordered layers. These layers form a dynamically evolving holographic code whose sequential updates, each corresponding to one Planck-scale incorporation per Planck time, generate an internal spacetime as a holographic projection of a closed, quasi-hexagonally tessellated surface. The relation $R = 2M$ binds horizon growth directly to internal expansion, so the internal age of the emergent universe follows from the accumulated mass encoded on the horizon, yielding approximately 13.4 Gyr and predicting that the observable Hubble domain encloses roughly half of the total internal mass. Cosmic acceleration and the Hubble tension emerge naturally as manifestations of horizon-layer dynamics rather than as evidence for an independent dark-energy component.

Within this framework, the unphysical singularity of classical general relativity is replaced by a finite, null-ordered causal boundary that preserves unitarity, causal completeness, and holographic information flow. The black hole interior is no longer interpreted as a region of divergent curvature but as the causal termination of classical geometry, maintained by the evolving horizon itself. Bulk curvature reflects the elastic response of the holographic surface to local deficits in causal adjacency, so gravity appears as the macroscopic expression of finite causal capacity in the boundary code. Singularities are removed not by ad hoc regularization but by replacing them with a physically operative, dynamically maintained null surface that stores all degrees of freedom permitted by the holographic bound.

When the parent black hole possesses angular momentum, Kerr frame dragging imprints a global azimuthal phase gradient across the horizon lattice. This gradient biases the incorporation of co-rotating versus counter-rotating quanta, producing a small but cumulative chiral asymmetry that can seed matter–antimatter imbalance and define a preferred cosmic axis. The binary spin structure of Planck-scale dipoles on the horizon provides a geometric origin for fermionic spin-$\frac{1}{2}$, the Pauli exclusion principle, parity violation, and large-scale alignments observed in CMB multipoles and galaxy spins. Microscopic spin quantization and macroscopic cosmological anisotropy thus arise as different projections of the same Kerr-induced phase structure encoded on the holographic boundary.

At a deeper level, the horizon-layered framework unifies general relativity, holography, and quantum measurement under a single causal principle. The horizon functions as a stationary yet continually reconfigured causal lattice: radial incorporation adds new Planck-scale cells, while lateral null propagation across the near-hexagonal adjacency graph sustains coherence, radiation, motion, and gravitational clustering. The speed of light c appears as the invariant rate of lateral causal synchronization on this null surface. Spacetime, motion, and cosmic expansion emerge together from the sequential retessellation of a fundamentally still holographic boundary.

This causal–informational picture also offers a natural resolution of the vacuum energy problem. Vacuum energy corresponds to residual curvature arising from incomplete local redundancy in the horizon code and is dynamically diluted as new Planck cells are incorporated. Cosmic acceleration follows as a geometric response to increasing holographic capacity rather than from a fixed vacuum energy density.

While the classical singularity-based paradigm remains mathematically consistent within general relativity, the horizon-layered cosmology proposes a deeper, information-theoretic foundation. It preserves established predictions—gravitational waves, inspiral dynamics, and black hole thermodynamics—while replacing the unobservable interior with a physically defined causal boundary. Observable consequences such as Kerr-induced anisotropies, horizon-coherence effects, and holographic regulation of vacuum energy provide concrete avenues for future empirical tests.

Although the formulation presented here is primarily conceptual, it establishes a coherent architecture for quantitative development: realistic collapse geometries, spin-weighted tessellations, precise mappings between two-dimensional horizon structures and three-dimensional bulk fields, and numerical simulations of null-layer encoding. The central insight, however, can already be stated succinctly:

> **Black holes are not endpoints of collapse but generative horizons. Each horizon layers infalling matter into a null-ordered holographic code whose self-consistent projection forms an emergent** $(3{+}1)$**-dimensional universe. Our universe is not matter moving through a pre-existing spacetime, but the evolving relational pattern of a dynamically growing holographic surface—a causal code whose successive incorporations generate the very fabric of reality.**

References

[1] Hooft, G.: Dimensional reduction in quantum gravity. arXiv preprint gr-qc/9310026 (1993)

[2] Susskind, L.: The world as a hologram. Journal of Mathematical Physics **36**(11), 6377–6396 (1995)

[3] Thorne, K.S., Price, R.H., Macdonald, D.A.: Black Holes: The Membrane Paradigm. Yale University Press, New Haven (1986)

[4] Maldacena, J.M.: The large n limit of superconformal field theories and supergravity. Advances in Theoretical and Mathematical Physics **2**, 231–252 (1998) https://doi.org/10.4310/ATMP.1998.v2.n2.a1 hep-th/9711200

[5] Schwarzschild, K.: On the gravitational field of a mass point according to einstein's theory. arXiv preprint physics/9905030 (1999)

[6] Schutz, B.: A First Course in General Relativity, pp. 317–322. Cambridge university press, Cambridge (2022)

[7] Hafele, J.C., Keating, R.E.: Around-the-world atomic clocks: Observed relativistic time gains. Science **177**(4044), 168–170 (1972)

[8] Ashby, N.: Relativity in the global positioning system. Living Reviews in relativity **6**(1), 1–42 (2003)

[9] Chou, C.-w., Hume, D., Koelemeij, J., Wineland, D.J., Rosenband, T.: Frequency comparison of two high-accuracy al+ optical clocks. Physical review letters **104**(7), 070802 (2010)

[10] Bekenstein, J.D.: Black holes and entropy. Physical Review D **7**(8), 2333 (1973)

[11] Hawking, S.W.: Particle creation by black holes. Communications in mathematical physics **43**(3), 199–220 (1975)

[12] Sperhake, U.: General Relativity 2: Lecture Notes. University of Cambridge. https://www.damtp.cam.ac.uk/user/us248/Lectures/Notes/grII.pdf (2016)

[13] Carroll, S.M.: An introduction to general relativity: spacetime and geometry. Addison Wesley **101**, 102 (2004)

[14] Aristotle: Physics

[15] Ashtekar, A., Bojowald, M.: Black hole evaporation: A paradigm. Classical and Quantum Gravity **22**(16), 3349–3362 (2005) https://doi.org/10.1088/0264-9381/22/16/014 arXiv:gr-qc/0504029

[16] Hajicek, P., Kiefer, C.: Singularity avoidance by collapsing shells in quantum gravity. International Journal of Modern Physics D **10**(06), 775–779 (2001) https://doi.org/10.1142/S0218271801001118 arXiv:gr-qc/0107102

[17] Barceló, C., Liberati, S., Visser, M.: Horizon thermodynamics and emergent gravity. International Journal of Modern Physics D **20**(08), 1667–1676 (2011) https://doi.org/10.1142/S0218271811019341 arXiv:0909.4157 [gr-qc]

[18] Mazur, P.O., Mottola, E.: Gravitational vacuum condensate stars. Proceedings of the National Academy of Sciences **101**(26), 9545–9550 (2004) https://doi.org/10.1073/pnas.0402717101 arXiv:gr-qc/0407075

[19] Almheiri, A., Marolf, D., Polchinski, J., Sully, J.: Black holes: complementarity or firewalls? Journal of High Energy Physics **2013**(2), 62 (2013) https://doi.org/10.1007/JHEP02(2013)062 arXiv:1207.3123 [hep-th]

[20] Misner, C.W., Thorne, K.S., Wheeler, J.A.: Gravitation. Macmillan, San Francisco (1973)

[21] O'Connor, E., Ott, C.D.: Black hole formation in failing core-collapse supernovae. The Astrophysical Journal **730**(2), 70 (2011)

[22] Shapiro, S.L., Teukolsky, S.A.: Black Holes, White Dwarfs and Neutron Stars: the Physics of Compact Objects. John Wiley & Sons, New York (2024)

[23] Woosley, S., Wilson, J., Mathews, G., Hoffman, R., Meyer, B.: The r-process and neutrino-heated supernova ejecta. Astrophysical Journal, Part 1 (ISSN 0004-637X), vol. 433, no. 1, p. 229-246 **433**, 229–246 (1994)

[24] Bousso, R.: A covariant entropy conjecture. Journal of High Energy Physics **1999**(07), 004 (1999)

[25] Hawking, S.W., Ellis, G.F.: The Large Scale Structure of Space-time. Cambridge university press, Cambridge, New York, Melbourne (2023)

[26] Guth, A.H.: Inflationary universe: A possible solution to the horizon and flatness problems. Physical Review D **23**(2), 347–356 (1981) https://doi.org/10.1103/PhysRevD.23.347

[27] Linde, A.D.: A new inflationary universe scenario: A possible solution of the horizon, flatness, homogeneity, isotropy and primordial monopole problems. Physics Letters B **108**(6), 389–393 (1982) https://doi.org/10.1016/0370-2693(82)91219-9

[28] Riess, A.G., Yuan, W., Macri, L.M., Scolnic, D., Brout, D., Casertano, S., Jones, D.O., Murakami, Y., Peterson, R., Polin, A., *et al.*: A comprehensive measurement of the local value of the hubble constant with 1 km/s/mpc uncertainty

from the hubble space telescope and the sh0es team. The Astrophysical Journal Letters **934**(1), 7 (2022) https://doi.org/10.3847/2041-8213/ac5c5b

[29] Gibbons, G.W., Hawking, S.W.: Cosmological event horizons, thermodynamics, and particle creation. Physical Review D **15**(10), 2738–2751 (1977)

[30] Padmanabhan, T.: Thermodynamical aspects of gravity: new insights. Reports on Progress in Physics **73**(4), 046901 (2010)

[31] Verlinde, E.: On the origin of gravity and the laws of newton. Journal of High Energy Physics **2011**(4), 1–27 (2011)

[32] Li, M.: A model of holographic dark energy. Physics Letters B **603**(1-2), 1–5 (2004)

[33] Smolin, L.: The Life of the Cosmos. Oxford University Press, New York - Oxford (1997)

[34] Frolov, V., Novikov, I.: Black Hole Physics: Basic Concepts and New Developments vol. 96. Springer, Dordrecht (2012)